





The long road of functional recruitment—The evolution of a gene duplicate to pyrrolizidine alkaloid biosynthesis in the morning glories (Convolvulaceae)

Arunraj Saranya Prakashrao¹ | Till Beuerle² | Ana Rita G. Simões^{3,4}  |
 Christina Hopf⁵  | Serhat Sezai Çiçek⁶  | Thomas Stegemann¹  |
 Dietrich Ober¹ | Elisabeth Kaltenecker¹ 

¹Department Biochemical Ecology and Molecular Evolution, Botanical Institute, Christian-Albrechts-University, Kiel, Germany

²Institute of Pharmaceutical Biology, Technische Universität Braunschweig, Braunschweig, Germany

³Royal Botanic Gardens, Kew, Richmond, UK

⁴Systematic and Evolutionary Botany Lab, Ghent University, Ghent, Belgium

⁵Department of Structural Biology, Zoological Institute, Christian-Albrechts-University, Kiel, Germany

⁶Department of Pharmaceutical Biology, Pharmaceutical Institute, Christian-Albrechts-University, Kiel, Germany

Correspondence

Elisabeth Kaltenecker, Department Biochemical Ecology and Molecular Evolution, Botanical Institute, Christian-Albrechts-University, Kiel, Germany.
 Email: ekaltenecker@bot.uni-kiel.de

Present address

Arunraj Saranya Prakashrao, Heart Research Center Göttingen, University Medical Center Göttingen, Göttingen, Germany.

Funding information

A-SP was funded by the International Max Planck Research School for Evolutionary Biology, Plön, Germany. Furthermore, A-SP was also supported by the FAZIT-STIFTUNG (Gemeinnützige Verlagsgesellschaft mbH).

Abstract

In plants, homospermidine synthase (HSS) is a pathway-specific enzyme initiating the biosynthesis of pyrrolizidine alkaloids (PAs), which function as a chemical defense against herbivores. In PA-producing Convolvulaceae (“morning glories”), HSS originated from deoxyhypusine synthase at least >50 to 75 million years ago via a gene duplication event and subsequent functional diversification. To study the recruitment of this ancient gene duplicate to PA biosynthesis, the presence of putative *hss* gene copies in 11 Convolvulaceae species was analyzed. Additionally, various plant parts from seven of these species were screened for the presence of PAs. Although all of these species possess a putative *hss* copy, PAs could only be detected in roots of *Ipomoea neei* (Spreng.) O’Donell and *Distimake quinquefolius* (L.) A.R. Simões & Staples in this study. A precursor of PAs was detected in roots of *Ipomoea alba* L. Thus, despite sharing high sequence identities, the presence of an *hss* gene copy does not correlate with PA accumulation in particular species of Convolvulaceae. In vitro activity assays of the encoded enzymes revealed a broad spectrum of enzyme activity, further emphasizing a functional diversity of the *hss* gene copies. A recently identified HSS specific amino acid motif seems to be important for the loss of the ancestral protein function—the activation of the eukaryotic initiation factor 5A (eIF5A). Thus, the motif might be indicative for a change of function but allows not to predict the new function. This emphasizes the challenges in annotating functions for duplicates, even for duplicates from closely related species.

KEYWORDS

deoxyhypusine synthase, *Distimake*, gene duplication, homospermidine synthase, *Ipomoea*, molecular evolution, pyrrolizidine alkaloids

List of Abbreviations: cDNA, complementary DNA; DHS, deoxyhypusine synthase; FPNI-PCR, fusion primer and nested integrated PCR; GC, gas chromatography; gDNA, genomic DNA; HSS, homospermidine synthase; MS, mass spectrometry; NAD, nicotinamide adenine dinucleotide; PAs, pyrrolizidine alkaloids; PCR, polymerase chain reaction; RACE, rapid amplification of cDNA ends; SEC-MALS, size-exclusion chromatography coupled to multi-angle light scattering.

This is an open access article under the terms of the [Creative Commons Attribution-NonCommercial-NoDerivs](https://creativecommons.org/licenses/by-nc-nd/4.0/) License, which permits use and distribution in any medium, provided the original work is properly cited, the use is non-commercial and no modifications or adaptations are made.

© 2022 The Authors. *Plant Direct* published by American Society of Plant Biologists and the Society for Experimental Biology and John Wiley & Sons Ltd.

1 | INTRODUCTION

Convolvulaceae, also known as “morning glories” or the “sweet potato” family, is a diverse group of flowering plants, with 60 genera and approximately 1800 species, widely distributed across the tropics, with fewer representatives in temperate regions (WCVP, 2021). This family has great economic importance, especially as food (“sweet potato” and “water spinach”) and ornamental plants (“bindweeds” and “morning glories”) and also for medicinal purpose (Chen et al., 2018). Based on molecular phylogenetic studies, the family has been classified into six monophyletic subfamilies (Figure 1a), among which Convolvuloideae is the most taxonomically diverse and economically important, including the tribes Ipomoeae, Merremieae and Convolvuleae (Stefanović et al., 2003). Many species of Convolvulaceae form a symbiosis with fungal endosymbionts (*Periglandula*

U. Steiner, E. Leistner & Leuchtm.), leading to the accumulation of ergot alkaloids in their seeds (Beaulieu et al., 2021; Leistner & Steiner, 2018). In consequence, the seeds of some species such as *Argyria nervosa* (Burm.f.) Bojer are well known natural psychotropics (Paulke et al., 2013). Furthermore, a number of species of the Convolvuloideae subfamily are known to produce pyrrolizidine alkaloids (PAs, Figure 1b; Eich, 2008). PAs are specialized metabolites produced in plants as part of their chemical defense against insect herbivores (Dreyer et al., 1985; Hartmann, 1999; Hartmann & Ober, 2008; Reinhard et al., 2009). PAs are also toxic to mammals including humans (Wiedenfeld & Edgar, 2011). Therefore, they have an economic impact as they can cross-contaminate food products such as honey, herbal drugs, and tea (Kaltner et al., 2018). PAs are also produced by other plant families, like the Asteraceae, Boraginaceae, Fabaceae, and Orchidaceae (Langel et al., 2011). To date, more than

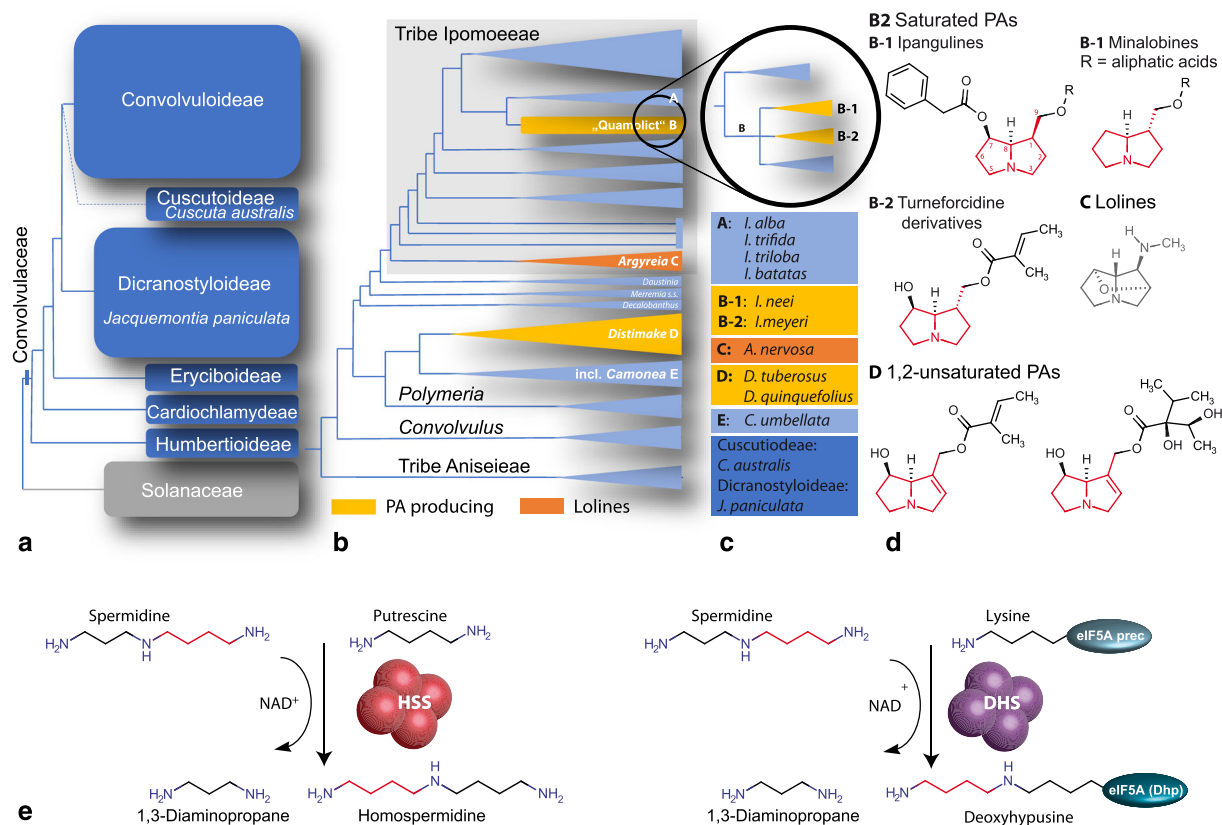


FIGURE 1 Pyrrolizidine alkaloids (PAs) occurring in the Convolvulaceae. (a) The figure illustrates the phylogenetic tree topology of the Convolvulaceae including the Solanaceae being its sister family. Species analyzed in this study all belong to the Convolvuloideae subfamily, except *Cuscuta australis* (Cuscutoidae), and *Jacquemontia paniculata* (Dicanostyloideae). (b) Tree topology of the Convolvuloideae. Groups within the Convolvuloideae, which comprise single species that produce PAs and lolines, are highlighted. Abbreviations: incl. = including. (c) Species included in this study and their affiliation to the phylogenetic groups given in (a) and (b). (d) Structures of PAs and lolines, which have been detected in individual species. The characteristic core structure of PAs, the necine base, is given in red. Ipangulines and Minalobines with a saturated necine base occur in species that belong to the “B2-1”-clade within the “Quamoclit” clade (B2) that includes species previously assigned to subgenus Quamoclit, or closely related to it (sensu Austin, 1979), as demonstrated by recent molecular phylogenetic results (Muñoz-Rodríguez et al., 2019). In *Ipomoea meyeri*, which belongs to a sister group within this clade (B2-2), unsaturated turneforcidine derivatives have been found (Eich, 2008; Tofern, 1999). Lolines have been described to occur in *Argyria mollis* (Tofern et al., 1999). And finally, alkaloids that possess a 1,2-unsaturated necine base occur in *Distimake quinquefolius* and *Distimake cissoides* (Eich, 2008; Mann, 1997). (e) Main reactions catalyzed by homospermidine synthase (HSS) and deoxyhypusine synthase (DHS). While HSS preferentially catalyzes the transfer of an aminobutyl moiety (highlighted in red) from spermidine to putrescine, DHS favors a specific lysine of the eIF5A precursor as aminobutyl acceptor to form deoxyhypusine.



400 PAs have been identified (Langel et al., 2011). Despite this structural diversity, all PAs share a common base structure, namely a nitrogen-containing bicyclic ring system called necine base that is esterified with one or more “necic” acids (Figure 1d). Homospermidine is the precursor for the biosynthesis of the necine base (Böttcher et al., 1994) and is synthesized from putrescine and spermidine, which are part of the polyamine pool of plants. In PA-producing plants, homospermidine is formed by the homospermidine synthase (HSS, EC 2.5.1.45), which is considered to be the first pathway-specific enzyme of PA biosynthesis (Ober & Hartmann, 1999b; Ober, Harms, et al., 2003). In the presence of NAD^+ , HSS catalyzes the transfer of the aminobutyl moiety from spermidine to putrescine to form homospermidine (Ober & Hartmann, 1999b; Ober, Harms, et al., 2003, Figure 1e). Sequence-based homology studies have shown that HSS evolved via a gene duplication from deoxyhypusine synthase (DHS), which is involved in the first step of the post-translational activation of the eukaryotic translation initiation factor 5A (eIF5A, Ober & Hartmann, 1999b). DHS is a ubiquitous enzyme in eukaryotes and is essential for cell growth and viability (Chattopadhyay et al., 2008). Enzymatically, DHS and HSS perform an analogous reaction by transferring the aminobutyl group from spermidine to an acceptor. The difference lies in the specificity toward their respective aminobutyl acceptor. The DHS favors a specific lysine residue of the eIF5A precursor protein and catalyzes its modification to deoxyhypusine (DHS activity), while the HSS utilizes the polyamine putrescine (Figure 1e). Of note, the DHS is promiscuous and accepts various polyamines including putrescine as aminobutyl acceptor in the absence of the eIF5A precursor (Kaltenegger et al., 2021; Ober, Harms, et al., 2003; Park et al., 2003; Wątor et al., 2020; Wolff et al., 1997). Minor amounts of homospermidine, attributable to this side activity of the DHS, are found in many diverse plant species (Ober, Gibas, et al., 2003). However, in a *hss* knock out plant of *Symphytum officinale*, these low amounts of homospermidine as side-product of DHS are not channeled into PA biosynthesis (Zakaria et al., 2021).

HSS in PA producing species lost the ability to use the eIF5A precursor protein (Kaltenegger et al., 2013, 2021; Ober, Harms, et al., 2003). This change of function of HSS has been explained as an evolutionary adaptation of one of the gene copies and as a prerequisite for the recruitment to PA biosynthesis (Reimann et al., 2004). Interestingly, the recruitment of HSS from DHS occurred multiple times after the independent gene duplication events in PA-producing plant lineages (Reimann et al., 2004). However, Convolvulaceae represent a special case, since the PAs detected in Convolvuloideae subfamily can be assigned to two different types. First, PAs with a saturated necine base including unique types of PAs known as ipangulines, minalobines and turnefordicine derivatives (Figure 1d, Jenett-Siems et al., 1993; Jenett-Siems et al., 1998; Jenett-Siems et al., 2005; Tofern, 1999; Eich, 2008) occur in several species of the “Quamoclit” clade of *Ipomoea* L. (Figure 1b, clade B2-1) and in *Ipomoea meyeri* (Spreng.) G. Don, located in the sister clade of the “Quamoclit” clade (Figure 1b, clade B2-2, Muñoz-Rodríguez et al., 2019). Second, 1,2-unsaturated PAs (Figure 1d) have been described for *Distimake quinquefolius*

(L.) A.R.Simões & Staples (syn. *Merremia quinquefolia*) and *Distimake cissoides* (Lam.) A.R.Simões & Staples (syn. *Merremia cissoides*) (Figure 1b, clade G, Eich, 2008; Mann, 1997). Noteworthy is also the occurrence of lolines in *Argyrea mollis* (Burm. f.) Choisy (Tofern et al., 1999). Lolines (Figure 1d), though having a backbone structure that is similar to the necine base, are biogenetically unrelated to PAs (Hartmann & Witte, 1995; Schardl et al., 2007).

The occurrence of two different structural types of PAs in *Ipomoea* L. and *Distimake* Raf. suggests their independent evolutionary origin. Surprisingly, the HSS in both lineages originated from a single gene duplication (Kaltenegger et al., 2013), which occurred prior to the divergence of the Ipomoeae and the clade that includes *Distimake* and allied genera, roughly 75 to 50 million years ago (mya) (Eserman et al., 2014). As the last common ancestor of both groups possessed a putative *hss* gene copy, it could theoretically have been inherited by all of its descendants. We have thus hypothesized that the *hss* gene copy is widespread in species of the entire Convolvuloideae and that it might have been recruited for PA biosynthesis in further species. Indeed, an ortholog of HSS has also been found in *Convolvulus arvensis* L., but this ortholog shows clear signs of being a pseudogene (Kaltenegger et al., 2013). Additionally, *Ipomoea alba* L., which belongs to a sister clade of the “Quamoclit” clade of *Ipomoea* (Figure 1b), possesses an ortholog of HSS, but its function is unknown (Kaltenegger et al., 2013).

To gain more insight, we studied the presence of putative *hss* genes in further species of subfamily Convolvuloideae and in parallel screened for the occurrence of PAs (Figure 1c and Table S1), namely, in a selection of representatives of Ipomoeae (*A. nervosa*, *I. alba*) and the genera *Distimake* [*Distimake tuberosus* (syn. *Merremia tuberosa*)] and *Camonea* Raf. [*Camonea umbellata* (syn. *Merremia umbellata*)], which were previously assigned to the genus *Merremia* Dennst. ex. Endl., but have now been recognized as distinctive based on molecular, morphological and biogeographic data (Simões et al., 2015; Simões & Staples, 2017). As positive control, we also analyzed *Ipomoea neei* and *D. quinquefolius* (syn. *M. quinquefolia*) for PAs. For comparison reasons, we screened representatives of the subfamilies Dicranostyloideae (*Jacquemontia paniculata* (Burm.f.) Hallier f.) and Cuscutioideae (*Cuscuta australis* Hook.f.) for the presence of *hss* gene copies. Due to its use as crop plant, we also included *Ipomoea batatas* and its ancestral species *Ipomoea trifida* and *Ipomoea triloba* in this screen.

2 | RESULTS

2.1 | Identifying homologs of *dhs* and *hss* in Convolvulaceae

For every species, except *J. paniculata*, we were able to amplify two *dhs* homologs from genomic or cDNA (Table S2). The amplified sequences varied in length and covered the partial open reading frame (ORF) or, in five out of nine sequences, the complete ORF (Table S4). Additionally, we obtained sequences homologous to *dhs* from the



TABLE 1 Pairwise sequence identity among DHS and HSS sequences (cDNA) from the Convolvulaceae

No.	Species	1	2	3	4	5	6	7	8	9	10	11	12	13	14	15	16	17	18	19	20	21	
1	DHS <i>Cuscuta australis</i>																						
2	DHS <i>Justicia paniculata</i>	87.1																					
3	DHS <i>Campona umbellata</i>	86.8	88.4																				
4	DHS <i>Argyria nervosa</i>	86.5	87.6	94.7																			
5	DHS <i>Ipomoea batatas</i>	86.7	87.6	95.7	96.8																		
6	DHS <i>Ipomoea trifida</i>	86.2	87	95.1	96.2	99																	
7	DHS <i>Ipomoea triloba</i>	87.2	87.6	95.7	96.3	98.8	98.4																
8	DHS <i>Ipomoea alba</i>	86.4	87.4	94.6	96.3	98.1	97.6	97.4															
9	DHS <i>Ipomoea neei</i>	86.2	87	94.7	95.5	97.6	96.9	97.2	97.2														
10	DHS <i>Dichotomosiphon tuberosus</i>	88.7	93.4	96.6	95.4	96.4	95.7	96.1	95.4	95.4													
11	DHS <i>Distimake quinquefolius 1</i>	87.2	87.9	96.2	94.5	95.4	95.1	95.2	94.5	94	96.6												
12	DHS <i>Distimake quinquefolius 2</i>	87	87.9	96.2	94.3	95.2	94.9	95	94.3	93.8	96.4	99.7											
13	HSS <i>C. umbellata</i>	84.5	85.9	90.3	88.8	89.9	89.3	89.8	89.7	89.5	91.9	90.4	90.4										
14	HSS <i>A. nervosa</i>	83.2	82.8	88.1	87.5	87.6	87.2	87.9	88	87.6	89.6	87.8	87.6	89.6									
15	HSS <i>I. trifida</i>	82.5	82.7	86.7	86.8	86.9	86.4	86.8	86.9	86.3	88.9	86.9	86.7	90.3	92.7								
16	HSS <i>I. triloba</i>	82.4	81.2	86.4	86.2	86.5	86	86.5	86.3	86	89.1	86.3	86.1	89.6	92.5	97.8							
17	HSS <i>I. alba</i>	82.7	81.9	86	86.3	86.2	85.9	86.6	86.2	85.8	89.2	86	85.8	89.2	91.7	93.4	93.5						
18	HSS <i>I. neei</i>	81.9	81.6	85.8	85.6	85.8	85.4	86	85.9	85.5	88.6	85.9	85.7	89.5	92.4	94.5	94.1	95.1					
19	HSS <i>D. tuberosus</i>	86.2	89.9	85.1	84.2	85.4	84.8	85.2	84.6	84.7	90.9	85	84.8	87.1	85.4	85.3	84.2	85.4	84.8				
20	HSS <i>D. quinquefolius 1</i>	82.8	82.5	86.5	85.4	86.5	86	86.5	85.7	85.7	88.2	86.5	86.3	90	87.8	88.4	88.1	87.7	88	88.3			
21	HSS <i>D. quinquefolius 2</i>	81.8	81.6	84.7	84.1	84.8	84.4	84.8	84.3	84.1	86.8	84.7	84.7	87.8	86.3	86.9	86.8	85.5	86.7	86.8	86.8	92.6	

Note: The sequences were identified as deoxyhypusine synthase (DHS) and homospermidine synthase (HSS) according to their position in the phylogenetic tree. Percentage of positions are shown where two sequences have an identical base or residue. Colors highlight the pairwise sequence identities of DHS versus DHS (gray) and of HSS versus HSS (orange).

genomes of *I. trifida* (Kunth) G. Don, *I. triloba* L., and *I. batatas* L. (Table S4). The average length of the ORF was about 1140 bp. In pairwise sequence comparisons, including the previously published DHS- and HSS-coding sequences from *I. neei*, *I. alba*, and *D. quinquefolius* (Kaltenegger et al., 2013), the sequences showed a high degree of identity from 83.6% to 99.7% (Table 1). Highest pairwise sequence identity was found between the putative DHS sequences from the two *D. quinquefolius* individuals. GenBank accession numbers are given in Table S4.

However, based on sequence data alone, DHS- and HSS-coding sequences cannot be differentiated. Thus, to further distinguish the newly identified sequences in *dhs* and *hss* orthologs, their phylogeny was reconstructed by calculating a maximum likelihood tree. Only the coding regions were used for the analysis. The DHS-encoding sequences of representatives of Solanaceae (sister family to Convolvulaceae in the order Solanales)—*Nicotiana tabacum* L. and *Solanum lycopersicum* L. (syn. *Lycopersicon esculentum*)—were included as outgroup. The resulting phylogenetic tree showed a clear bifurcation with two main clades (Figure 2a), and the branching pattern within both clades was mainly consistent with the topology of the currently published species trees of the Convolvulaceae (Eserman et al., 2014; Muñoz-Rodríguez et al., 2019; Simões et al., 2015; Stefanovic et al., 2002). Based on the previously biochemically characterized sequences from *I. neei*, *I. alba*, and *D. quinquefolius*, the two main clades could be classified as DHS- and HSS-coding clades (Figure 2a). Thus, the phylogeny added evidence to the previously described

single gene duplication event of the *dhs* in the Convolvulaceae (Kaltenegger et al., 2013). Furthermore, as the DHS from *C. australis* and *J. paniculata* are sister to Convolvuloideae DHS and HSS, the phylogeny suggests that the gene duplication occurred within the Convolvuloideae. The pairwise Ks distances between the paralogous DHS/HSS pairs range from 0.2 to 0.4 (Table S6).

In contrast to the highly conserved DHS clade, a longer branch length that indicated an increased nucleotide substitution rate between the individual *hss* sequences was observed in the HSS clade (Figure 2a) as previously described for the HSS sequences of the Boraginaceae and Asteraceae (Reimann et al., 2004).

Of note, all species of subfamily Convolvuloideae that were selected for this study possessed an ortholog in both clades, providing them with a putative HSS encoding gene copy to catalyze the first step in PA biosynthesis; while in species of the other subfamilies—*J. paniculata* (subfamily Dicranostyloideae) and *C. australis* (subfamily Cuscutioideae)—only a *dhs* gene copy was detected. As the sequences identified in this study were amplified from cDNA, except for *D. tuberosus* (Table S4), the genes also seem to be actively transcribed. Also, transcriptome profiles retrieved from the “Sweetpotato Genomics Resource” platform support that both genes, *dhs* as well as the putative *hss*, are transcribed in *I. triloba* as well as *I. trifida*. In detail, the *dhs* gene in *I. triloba* and *I. trifida* was found to be transcribed in flowers, flower buds, roots, leaves, and stems. The putative *hss* gene transcription profile differs only slightly, as the *hss* ortholog is supported to be strongest transcribed in flower buds but not in roots.

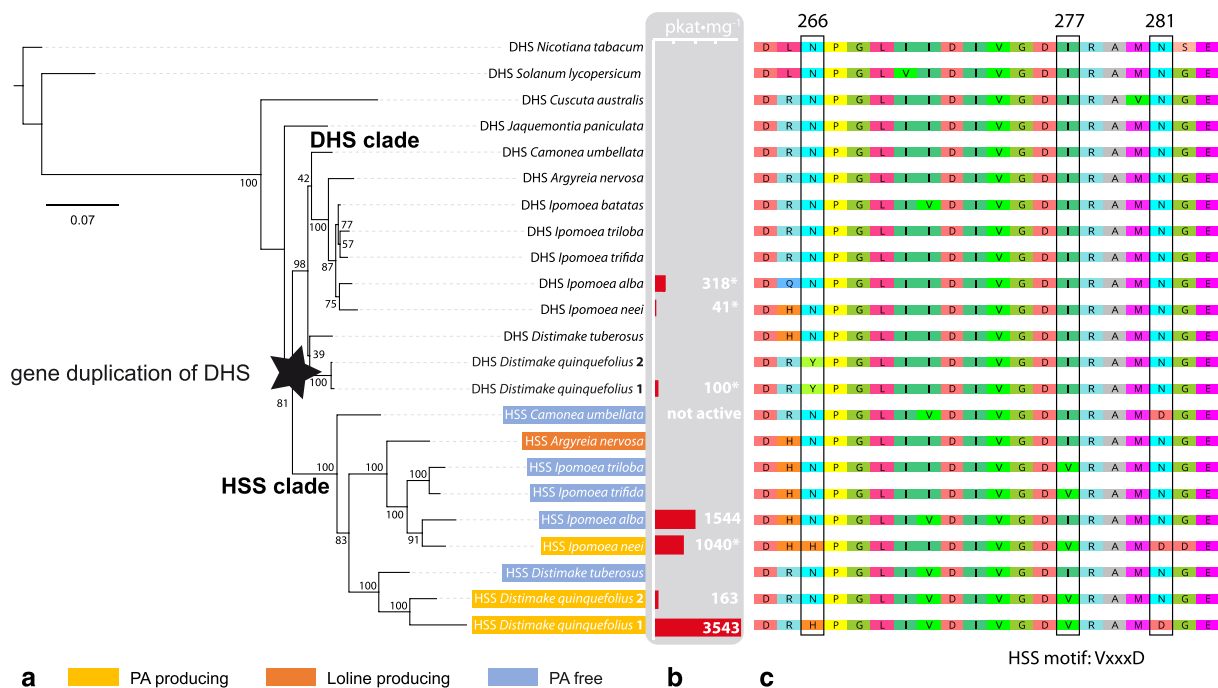


FIGURE 2 Phylogenetic analyses of deoxyhypusine synthase (DHS)- and homospermidine synthase (HSS)-encoding sequences. (a) A maximum likelihood tree was built from the cDNA sequences of HSS and DHS from the Convolvulaceae family and two DHS sequences from Solanaceae family. Percentages of bootstrap support values (for 1000 replicates) are indicated. The ancient duplication is highlighted, and the DHS and HSS clades are indicated. (b) Selected sequences were chosen for biochemical analyses of the encoded enzymes. The calculated specific activity (pkat·mg) of homospermidine production of these enzymes in glycine-based assay buffer is given (see Table 3). Specific activities marked with an asterisk were taken from a previous study (Kaltenegger et al., 2013) (c) Alignment of the functionally characterized “HSS motif” (H-V-D)

2.2 | Presence of PAs in the Convolvulaceae

Of the Convolvulaceae species studied here, *I. neei* and *D. quinquefolius* have been previously described as producing PAs (Eich, 2008; Jenett-Siems et al., 2005, 1998; Mann, 1997). Leaves, stems, and roots of these species, grown in the greenhouses of Kiel Botanic gardens, were analyzed in this study and served as positive control. In *I. neei*, PAs were mostly detected in the roots (Suppl. Table S5). In shoots, only traces of PAs were detected. The exact pattern of PAs was slightly different from that of previous studies (Jenett-Siems et al., 2005, 1998), as ipanguline C3 was identified to be the main component in the roots in this study and so far was not described to occur in *I. neei*. However, all PAs found in the roots belonged to the ipanguline/isoipanguline type (Figure 1a). Slight variations in the species-specific bouquet of PAs have previously been observed (Jenett-Siems et al., 2005, 1998). In roots of the two individuals of *D. quinquefolius*, 16 different retronecine-based PAs (Table 2) were detected. In agreement with Mann (1997), 9-angeloylretronecine was the main alkaloid. Further prominent compounds that have also been described by Mann (1997) were creatonotine B, and lycopsamine. Interestingly, creatonotine was first isolated and described from adults of the moth *Cretonotos transiens* Walker, which as larvae received retronecine or ester alkaloids in their diet (Hartmann et al., 1990) and is usually not found in plants itself. The specific bouquet of PAs in the roots of the two individuals is very similar; however, the total amount differs considerably, with individual 2 accumulating only half of the PAs compared to individual 1 (.58 versus 1.28 mg·g⁻¹ dry weight, Table 2).

We also screened leaves, stems and roots of the *hss*-possessing Convolvulaceae species *A. nervosa*, *I. alba*, *D. tuberosus*, and *C. umbellata* for the presence of PAs. In *I. alba*, the free necine base (trachelanthimidine and isoretronecanol, in a ratio 20:1) was detected in roots. However, in all other species, neither the free necine base nor PAs were detected.

2.3 | The ability of HSS from selected morning glories to produce homospermidine

As many Convolvulaceae possess an HSS ortholog, but do not produce PAs according to our analyses, we decided to test the ability of some of the newly identified HSS orthologs to produce homospermidine in vitro with a newly established non-radioactive activity assay (Kaltenegger et al., 2021). We chose the HSS from the PA-free *C. umbellata* (CuHSS) and the PA-producing *D. quinquefolius* individual 2 (*Dq2HSS*). Both differ in a previously described specific amino acid motif ("HSS motif": 277Vxxx281D, Figure 2c, Livshultz et al., 2018; Gill et al., 2018, the numbering follows Kaltenegger et al., 2013), that is shared by many HSS enzymes. They also differ in a third site (266H, Figure 2c), which was calculated to be positively selected in the PA producing *Ipomoea* species (Kaltenegger et al., 2013), providing an "extended" HSS motif

(H-VxxxD) in the morning glories. We also re-analyzed the abilities of the previously characterized HSS from *D. quinquefolius* individual 1 (*Dq1HSS*), which possesses the extended HSS motif, and the HSS from *I. alba*, lacking the motif (*laHSS*) (Kaltenegger et al., 2013). All four enzymes were successfully expressed and purified (Figure 3a). Size exclusion chromatography coupled with multi-angle light scattering (MALS) and an UV detector confirmed the tetrameric state of the purified proteins (Figure 3b), which corresponds to the biological active form of DHS and its homologs (Tanaka et al., 2020; Umland et al., 2004; Wątor et al., 2020). Only CuHSS showed an additional signal to the main peak in borate buffer, which size corresponds to a dimeric state of the enzyme and indicates a misassembly. In the in vitro activity assays, the *Dq2HSS* (N-VxxxN), was able to produce low amounts of homospermidine only in glycine buffer, and the specific activity of homospermidine formation was twentyfold lower (163 pkat·mg⁻¹, Table 3) compared to the specific activity of *Dq1HSS* (H-VxxxD, 3543 pkat·mg⁻¹). In contrast, the *laHSS*, lacking the motif, produced homospermidine in glycine and borate buffer (1544 pkat·mg⁻¹, 46 pkat·mg⁻¹, respectively). The CuHSS (N-lxxxD) did not produce homospermidine, neither in glycine nor borate buffer.

2.4 | The HSS motif and its effect on enzyme activity

Although *Dq1HSS* and *laHSS* differ in the HSS motif, they are both able to produce homospermidine. However, the presence of this motif might still be related to functional differences between the HSS. To get a better idea about this, their ability to use cadaverine and *N*-methylputrescine as putrescine analogs as well as spermine as spermidine analog was investigated (Table S7). Cadaverine could be used by both enzymes, thereby producing (4-aminobutyl)(5-aminopentyl)amine (Figure 3c), but *Dq1HSS* showed with 1510 pkat·mg⁻¹ higher activity compared to *laHSS* (215 pkat·mg⁻¹). Additionally, canavalmine was produced by using spermidine as aminobutyl donor and acceptor. However, 1,3-diaminopropane increased most prominently in this assay (*Dq1HSS* 3,111 pkat·mg⁻¹, *laHSS* 1,187 pkat·mg⁻¹), indicating that spermidine was cleaved to 1,3-diaminopropane and the aminobutyl moiety. The latter is assumed to spontaneously form Δ^1 -pyrroline, as described for human DHS (Wolff et al., 1990), hence could not be detected by the applied in vitro assay.

Neither *Dq1HSS* nor *laHSS* were able to use *N*-methylputrescine as aminobutyl acceptor but utilized spermidine instead. In parallel, spermidine cleavage occurred. Spermine was not utilized as donor of an aminopropyl moiety, although spermine is known to bind in the human DHS similar to spermidine (Wątor et al., 2020). Thus, the presence of the HSS motif did not strongly affect the polyamine substrate spectrum of *Dq1HSS* and *laHSS*. However, when incubated with the eIF5a precursor, only *laHSS* was able to use it as an acceptor for the aminobutyl moiety of spermidine thereby producing deoxyhypusine (Figure S2). We next introduced the HSS motif to *laHSS*

**TABLE 2** Pyrrolizidine alkaloids from the *Distimake quinquefolius* individuals

	Alkaloid	RI ZB1MS/ TG-5SILMS	[M] ⁺	<i>D. quinquefolius</i>		MS data: characteristic ions m/z (% relative abundance)	Ref.
				Ind. 1 root	Ind. 2 root		
1	Supinidine	1254/1294	139 (100)	6	30	139(100), 138(15), 122(55), 120(14), 111(21), 110(20), 108(43), 94(10), 80(82), 68(7)	c,d
2	Retronecine	1427/1484	155 (44)	52	22	155(44), 111(85), 110(6), 94(21), 93(8), 82(6), 81(12), 80(100), 68(12), 53(5)	c,e
3	7-Angeloylretronecine	1784/1829	237 (5)	11	22	219(8), 137(28), 136(23), 124(32), 111(45), 106(40), 94(23), 83(16), 81(12), 80(100), 55(20)	c,e
4	9-Angeloylretronecine	1792/1841	237(4)	260	207	219(2), 154(29), 138(49), 137(59), 136(15), 94(31), 93(100), 83(5), 80(9), 55(10), 53(3)	c,e
5	9-Seneciolyretronecine	1838/1883	237 (2)	8	6	219(1), 193 (4), 155(19), 154(20), 138(26), 137(38), 136(11), 94(26), 93(100), 83(14), 80(11), 67(3), 55(5)	c,e
6	Unknown PA	1851/1895	?	tr	tr	154(19), 138(19), 137(26), 94(25), 93(100), 80(14), 55(15)	—
7	Isocreatonotine B	1966/2016	269 (6)	50	8	251(26), 236(3), 234(3), 154(4), 138(68), 137(30), 136(17), 124(20), 120(29), 111(75), 106(56), 94(27), 93(12), 80(100), 68(13)	c,f
8	Creatonotine B	1984/2039	269 (2)	170	30	225(6), 139(10), 138(100), 137(14), 136(8), 94(23), 93(56), 80(7), 67(3), 57(2), 53(1)	c,f
9	Retronecine-9-ester	2038/2084	297 ^a (.53)	35	9	155(10), 138(31), 137(18), 136(13), 94(21), 93(100), 80(16), 67(6), 53(6)	—
10	7-Acetyl-creatonotine isomer	2083/2124	311 ^a (.60)	54	39	197(5), 181(11), 180(100), 136(23), 120(42), 119(17), 118(15), 101(16), 94(34), 93(80), 80(20), 67(11), 57(18)	—
11	Indicine/Intermedine	2133/2196	299 (2)	210	130	156(9), 139(37), 138(100), 137(11), 136(10), 120(7), 95(10), 94(35), 93(52), 80(7), 67(5)	c,e
12	Lycopsamine	2141/2202	299(2)	119	47	254(2)n 156(9), 139(33), 138(100), 137(11), 136(9), 120(8), 95(10), 94(36), 93(49), 80(7), 67(4)	c,e
13	Acetylcindicine/ Acetylintermedine	2219/2264	341 (.33)	tr	tr	181(26), 180(100), 152(8), 136(23), 121(23), 120(18), 119(18), 101(14), 94(29), 93(86), 80(29), 67(5)	—
14	Unknown 220 #1	2288/2339	?	tr	tr	237 (30), 220(19), 137(15), 136(100), 120(30), 119(26), 94(35), 93(42), 83(26), 55(39)	—
15	Unknown 220 #2	2352/2372	?	tr	tr	237(21), 221(21), 220(100), 136(90), 120(21), 119(22), 93(20), 83(22), 57(18)	—
16	Unknown 220 #3	2500/2396	351 ^a (.86)	57	13	220(100), 136(97), 120(42), 119(30), 94(41), 93(70), 83(70), 55(22)	—
Total PAs ($\mu\text{g g}^{-1}$ dry weight): ^b				1029	561		

Note: The columns show the name of the alkaloid, the linear retention index (RI) for TG-1MS and TG-5SILMS columns, respectively, the molecular ion [M]⁺, the abundance, mass spectra of the identified PA, and the spectral references.

^aPutative [M]⁺ ion, estimated based on the mass spectrum.

^bHeliotrine equivalents based on GC-FID quantification.

^cIn house database of pyrrolizidine alkaloids: MS and linear retention index data.

^dKelley RB, Seiber JN. Pyrrolizidine alkaloid chemosystematics in *Amsinckia*. *Phytochemistry*. 1992; 31:2369–87.

^eWitte L, Rubiolo P, Bicchi C, Hartmann T. Comparative analysis of pyrrolizidine alkaloids from natural sources by gas chromatography–mass spectrometry. *Phytochemistry*. 1992; 32:187–96.

^fHartmann T, Theuring C, Beuerle T, Ernst L, Singer MS, Bernays EA. Acquired and partially de novo synthesized pyrrolizidine alkaloids in two polyphagous arctiids and the alkaloid profiles of their larval food-plants. *J Chem Ecol*. 2004; 30:229–54.

via site-directed mutagenesis and biochemically characterized the single mutants N266H, I277V, and N281D as well as a triple mutant with a fully introduced HSS motif for their activity with putrescine (HSS activity) as well as the eIF5a precursor. While the

homospermidine producing activity was highly similar, the N281D and triple mutant showed no activity with the eIF5a precursor (Figure S2). Thus, the motif could be a diagnostic marker for the loss of the DHS activity.

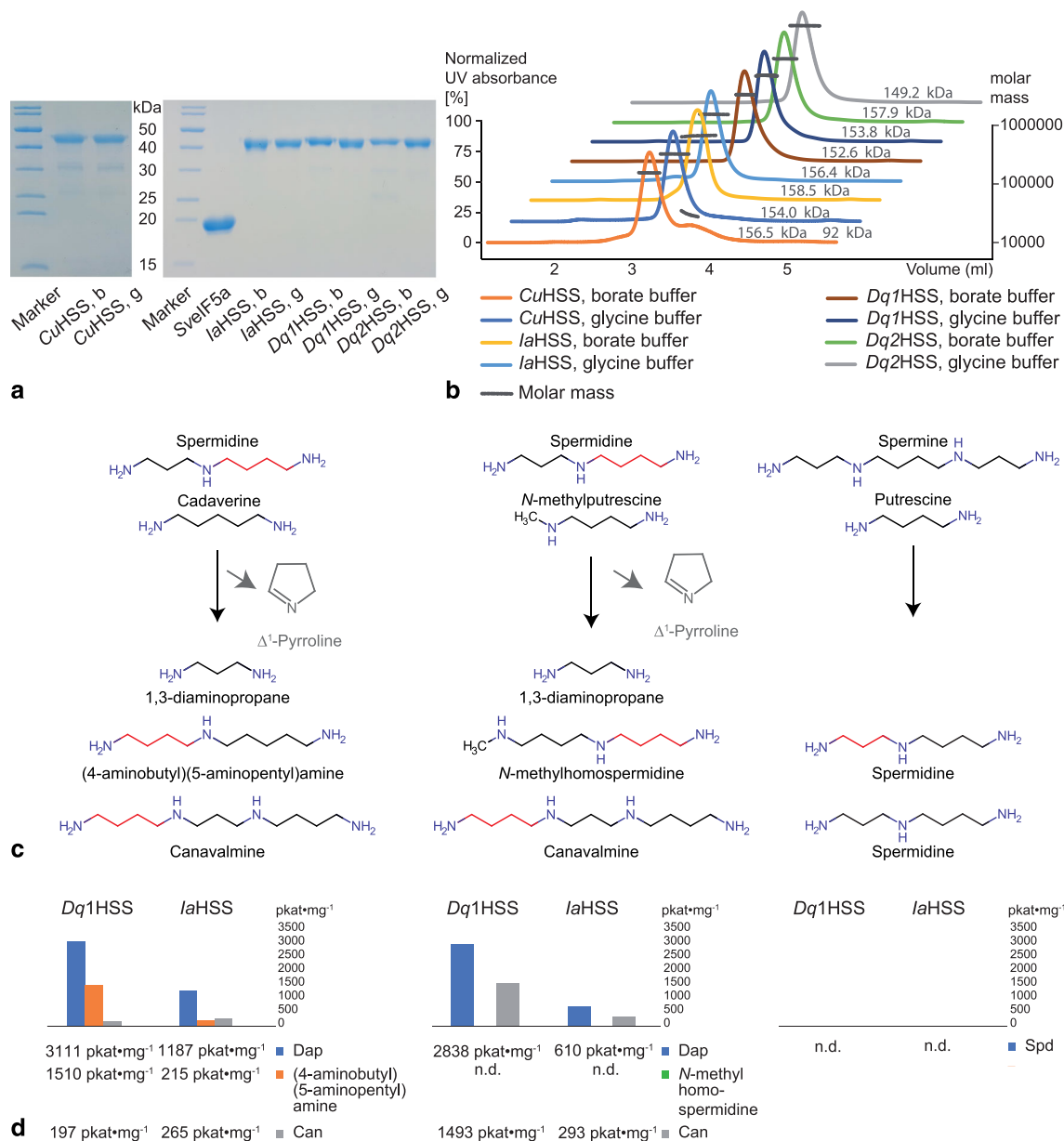


FIGURE 3 Heterologously expressed and purified HSS enzymes and their biosynthetic activity. (a) A PageBlue stained SDS-polyacryl gel of the purified and concentrated CuHSS (41.9 kDa), Dq2HSS (42.1 kDa), Dq1HSS (41.3 kDa), IaHSS (41.5 kDa) in borate (b) and glycine (g) buffer and the *Senecio vernalis* eIF5A precursor protein (18.3 kDa) is shown. (b) SEC-MALS/UV confirmed the tetrameric state (~150 kDa) of purified HSS enzymes. Only CuHSS in borate buffer shows a second signal of 92 kDa, indicating misassembly. (c) Potential reactions catalyzed by homospermidine synthase (HSS). If the polyamines cadaverine and *N*-methylputrescine are accepted as aminobutyl acceptors from the donor spermidine, (4-aminobutyl)(5-aminopentyl)amine and *N*-methylhomospermidine, respectively, would be formed with 1,3-diaminopropane as byproduct. Potential side reactions include the transfer from aminobutyl to spermidine, yielding canavalmine, and the sole spermidine cleavage, yielding 1,3-diaminopropane and Δ^1 -Pyrroline. If spermine can be utilized as aminopropyl donor with putrescine as acceptor, spermidine would be formed. (d) The observed specific activities of Dq1HSS and IaHSS in *in vitro* activity assays with the substrates depicted in (c). Abbreviations: Can, Canavalmine; Dap, 1,3-Diaminopropane; Spd, Spermidine

2.5 | The active site between DHS and HSS enzymes is highly conserved

In the course of this study, homology models of DHS and HSS of *I. alba*, *I. neei*, *D. quinquefolius*, and *C. umbellata* were generated based on an available high-resolution structure from human DHS

(Figures 4b–d and S3). Due to its mobility, the *N*-terminal part, which forms the so-called ball-and-chain-motif in human DHS (Umland et al., 2004), was not included. According to these homology models, HSS as well as DHS enzymes from the Convolvulaceae share a highly conserved 3D structure (Figure 4b). This is especially true for the active sites, which are located at the interface of the A-B and C-D

TABLE 3 Specific activities of HSS encoding cDNA sequences from various Convolvulaceae species

Species	Specific activity (pkat·mg ⁻¹)			PA type
	Glycine buffer	Borate buffer	PAs	
<i>Ipomoea neei</i>	1040*	n.a.	+	lpangulines
<i>Ipomoea alba</i>	1544 (12%)	46 (13%)	–	Necine base
<i>Distimake quinquefolius</i> ind. 1	3543 (3%)	482 (6%)	+	Lycopsamine
<i>D. quinquefolius</i> ind. 2	163 (23%)	Not active	+	Lycopsamine
<i>Camonea umbellata</i>	Not active	Not active	–	–

Note: The enzymes ability to produce homospermidine in glycine- and borate-based assay buffer is given. In bracket, relative standard deviation of three assays are given. Specific activities labeled with an asterisk (*) refer to Kaltenecker et al. (2013).

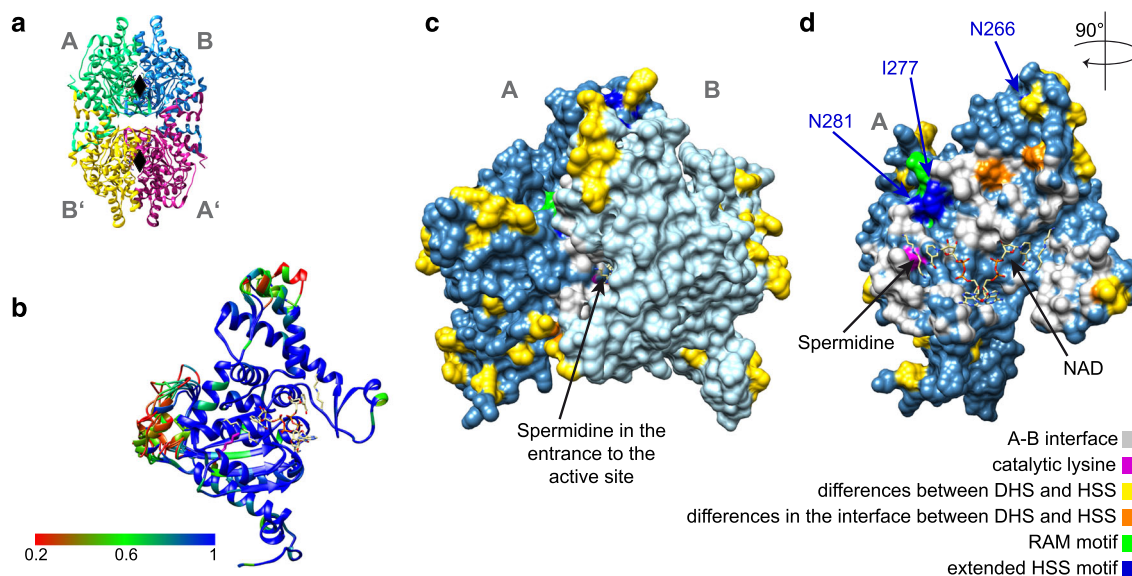


FIGURE 4 Homology models of homospermidine synthase (HSS) and deoxyhypusine synthase (DHS). Spermidine and nicotinamide adenine dinucleotide (NAD) are shown as sticks, colored by heteroatom. The N-terminal “ball-and-chain” motifs are omitted. (a) Ribbon representation of the human DHS tetramer (PDB: 6XXJ) with black diamonds indicating the general location of the active sites. The tetramer consists of two dimers (A-B, A'-B'), which comprise two antiparallel active sites at their interfaces. (b) Overlay of chain A of all DHS and HSS models in ribbon representation from *Ipomoeaalba*, *Ipomoea neei*, *Distimake quinquefolius* individuuum 1 and 2, *Camonea umbellata*, colored by residue identity from red = low identity to blue = high identity. The catalytic lysine is represented as purple stick. Spermidine and NAD from chain A and B are shown. (c,d) Surface representation of the A-B dimer and the A monomer from the *I. alba* HSS model, respectively. Residues that differ between the DHS and HSS pair from *I. alba* are colored in yellow, and in orange, if they are additionally located in the interface of the A-B dimer. The interface area of chain A is colored in light gray with the catalytic lysine in purple. The location of the extended HSS motif and the conserved RAM motif is highlighted.

homodimer and consist of residues from both subunits. All enzymes share the catalytically active Lys329 residue (numbering according to human DHS) (Figure 4c,d and S3), to which the aminobutyl moiety from spermidine is attached to form a transient enzyme-imine intermediate (Joe et al., 1997). Additionally, the sites that form hydrogen bonds or hydrophobic interactions with spermidine and NAD according to the crystal structure of human DHS (PDB ID 6XXJ, Wator et al., 2020) are conserved (Figure S1). Overall, in the interface region only very few residues vary between HSS enzymes and their respective DHS ancestors (Figure S3).

The sites of the putative HSS motif (277Vxxx281D) are located in the interface of the A-B dimer (Figure 4D, *Ia*HSS and Figure S3) in

close vicinity to but not as part of the active site. 266H of the extended motif is located in a loop above the interface, which is less conserved and flexible in the models. According to this location, none of the three sites seem to be directly involved in polyamine substrate or co-factor binding. The amino acids that are flanked by the HSS motif are highly conserved (RAM motif) and buried within the protein.

The electrostatic potential distribution at the entrance to the active-site tunnel was suggested to shape the interactions with the eIF5a precursor (Umland et al., 2004). In the morning glories, only some of the paralogous HSS/DHS pairs qualitatively differ. *Dq1*HSS and *Dq2*HSS are highly similar to their paralogous DHS counterparts but clearly show no activity with the eIF5A precursor (Figure S4).

Thus, changes of the polarity might be an important factor, but there are also other, yet not identified, factors.

3 | DISCUSSION

Our gene identification and phylogenetic analyses have shown that in many Convolvulaceae species a putative *hss* gene copy survived. According to our data, this gene originated from a gene duplication event prior to the divergence of Ipomoeae and the clade that includes *Distimake* and allied genera. In the genome of parasitic plant *C. australis*, only a *dhs* gene copy was identified. However, a massive gene loss has been described for *C. australis* (Sun et al., 2018). Thus, the *hss* copy might have been secondarily lost. To exactly date the gene duplication event, further species outside Convolvuloideae have to be analyzed. However, the available data support an ancient duplication event and imply a minimal retention time of the duplicated genes of around 75 to 50 million years based on the diversification of the Convolvuloideae (Eserman et al., 2014). The *Ks* distances between the paralogous pairs ranged from .2 to .4 (Table S6) and are in agreement with a postulated ancient gene duplication given that *Ks* distances vary among different gene families (Jiao et al., 2014) and between species (Qiao et al., 2019; Rausher et al., 1999; Wang et al., 2015). Many whole genome duplications that occurred 60 to 50 mya show *Ks* distances from .4 to 1.2 (Vanneste et al., 2014).

Although we have established a more widespread occurrence of the *hss* gene copy, we were not able to detect a similarly widespread occurrence of PAs, which agrees with previous studies of PAs in Convolvulaceae (Eich, 2008). In this study, PAs have been found only in roots of *D. quinquefolius* and *I. neei*, which are already known to produce PAs (Eich, 2008; Jenett-Siems et al., 2005; Mann, 1997). In *I. alba* (Figure 1b), traces of the unesterified necine base were detected in roots. One reason, why we could not detect PAs in further species might be that the individual plants that were investigated in this study lacked some necessary growing conditions or interaction partners during their cultivation. For example, a very specific regulation of PA biosynthesis by infection with rhizobial bacteria and nodulation has been reported in *Crotalaria* L. (Fabaceae, Irmer et al., 2015). A few studies report that tissue damage induced changes in the PA concentration like in *Jacobaea vulgaris* Gaertn. (syn. *Senecio jacobaea*) or *Cynoglossum officinale* L., but even without damage, high levels of PAs were present in these plants before (van Dam et al., 1993). Another explanation for the absence of PAs in the studied plants might be that not all individuals of one species produce PAs. Variations of the individual bouquet and the amount of PAs were detected in this study for *I. neei* and the two individuals of *D. quinquefolius*, but is also well documented for other PA-producing plants (Macel et al., 2004; Wesseling et al., 2017). These problems could be addressed by the screening of various individuals of one species for the presence of PAs. Sampling from diverse habitats might also be an important factor, especially as many Convolvulaceae have a pantropical distribution. Individuals from different geographic regions might differ in their PA production, as the herbivore community in these

various regions will also differ. However, in the majority of PA-producing plant families, PAs are considered to be part of the constitutive defense system of a plant (Hartmann, 1999). Furthermore, to our knowledge, no other study has reported the presence of PAs in other than the above mentioned Convolvulaceae species (Eich, 2008). Thus, we conclude that the presence of an *hss* gene copy does not correlate with the ability to produce PAs in the Convolvulaceae.

3.1 | Functional role of the *hss* gene copy

In many extant Convolvuloideae, *hss* orthologs were identified, but the fate of this duplicated gene might differ. In the PA-producing species, the duplicated copy diverged from the ancestor gene and gained a different substrate preference, thereby experiencing so-called *neo-functionalization*. Of course, further steps catalyzed by downstream enzymes are necessary to convert the reaction product of the HSS, that is, homospermidine, to generate a PA. While these additional catalytic enzymes are present in the PA-producing species, PA-free species simply might lack them. However, this raises the question why *hss* copies are still present in the PA-free species, after more than 50 million years? Several scenarios are possible. First, the gene copies are nonfunctional but have not been deleted yet. Becoming a pseudogene is considered to be the predominant fate of duplicates (Lynch & Conery, 2000). The half-life of duplicated genes varies greatly from two (Lynch & Conery, 2000) to approximately 30 million years and is influenced by many factors such as the mode of duplication, molecular and biological functions, and structural features (Panchy et al., 2016). The pseudogenization of a gene is mainly identified based on disabling mutations that lead to a loss of function but some pseudogenes in rice and *Arabidopsis* Heynh. have been shown to exhibit no clear signature of pseudogenization and are indeed expressed (Panchy et al., 2016). As for *hss* orthologs in the Convolvulaceae, two pseudogenes of the *hss* gene copy have been identified in *C. arvensis* L. (Kaltenegger et al., 2013) that bore clear marks of *non-functionalization*. The enzyme encoded by the *hss* gene from *C. umbellata* showed no activity with the tested substrates (Table 3). This gene might be a catalytically inactive paralog hence a pseudogene, but still the gene is present. Possibly, it survived solely by chance, as the presence of the redundant and thus useless gene copy was not deleterious enough for it to be efficiently purged from the genome (Koonin, 2016).

Second, PA biosynthesis might have been present in the ancestors but was secondarily lost in many extant Convolvuloideae species. *hss* gene copies would then be the remnants of a former functional pathway. *I. alba* takes an exceptional position, as it accumulates minor amounts of homospermidine and of the necine base but not complete PAs. Only recently, a copper-containing amine oxidase was identified to catalyze the second step in PA-biosynthesis in the PA-producing *Heliotropium indicum* L. (Zakaria et al., 2022). The reaction product has already the bicyclic ring system, characteristic for the necine base. Possibly, *I. alba* possesses an unoptimized amine oxidase and a primitive metabolic pathway to produce the necine base but lacks the necessary downstream enzymes and/or substrates to finalize the PA

biosynthesis. Such primitive metabolic pathway has also been described for morphinan biosynthesis in *Papaver rhoeas* L. (Yang et al., 2021). *I. alba* might be in a phase in which the pathway is evolving—or is in the process of losing the pathway.

A third explanation for the presence of the *hss* gene copy in PA-free species is their recruitment for a yet unidentified function. For example, unique indolizidine type alkaloids have been found in *I. alba* (Gourley et al., 1969). Lolines, which have a backbone structure that is similar to the necine base of PAs (Figure 1d), have been detected in *A. mollis* (Tofern et al., 1999). Further occurrence of lolines have been described in *Adenocarpus* DC. (Fabaceae) and grasses (Schardl et al., 2007). In the latter, a fungal endophyte has been shown to produce lolines (Schardl et al., 2007). Whether the lolines in the *Adenocarpus* and *Argyrea* species are of plant origin, or derived from endophytic fungi, has not been determined yet (Panaccione et al., 2014).

As a fourth alternative explanation, the structural features of the encoded protein favored their retention. The biologically active unit of HSS and DHS is a homotetramer (Figure 4). After duplication, the paralogs are predicted to interfere functionally and physically at the protein level. This so-called “paralog interference” is predicted to affect the fate of duplicates (Kaltenegger & Ober, 2015). For example, if degenerative mutations in one copy impact the activity, the gene product can still assemble with the intact subunits, and form less productive oligomers. Thus, degenerative mutations will be selected against, stabilizing both duplicates (Kaltenegger & Ober, 2015). For example, in *Trypanosoma brucei* DHS activity actually is dependent on heterotetramer formation between two DHS paralogs (Afanador et al., 2018).

In summary, the prediction of the function of a duplicated gene is an extremely difficult task. As we demonstrate here, even if a duplicated gene shows a dedicated function in several species, it might not have the same function (if any) in closely related species.

3.2 | Functional meaning of the “HSS motif”

The effects of mutations on protein properties are often unpredictable and mutations located far from binding or active sites can still dramatically affect protein function (Bershtein et al., 2021). The sites of the postulated HSS motif (266H-277Vxxx281D) are neither located in the four active sites of the tetramer nor at the entrance of the active site tunnel. Still, the presence of this HSS is functionally relevant, as it affects the activity with the eIF5a precursor. Even the single exchange of N281D in *la*HSS diminishes the activity with the eIF5a precursor. This agrees with the biochemical characterization of mutated DHS from *I. neei*, which was rendered to bear the HSS motif (Kaltenegger et al., 2013). Mutants bearing 281D of the HSS motif showed a significantly reduced DHS activity.

Epistasis between sites might be responsible for this phenomenon, as it is described, for example, in terpene synthases, in which many combinations of mutations outside the active site achieved a shift in the biosynthetic activity (OMaille et al., 2008). Furthermore, long-range contributions between the catalytic sites in heteromeric

DHS from *Trypanosoma brucei* have been described (Afanador et al., 2018). Additionally, the motif might affect not only substrate specificity but also protein stability and dimer formation, as the I277 and D281 are located in the interface of the A-B dimer (Figure 3b). CuHSS, having an intermediate motif, possibly forms less stable tetramers.

Though being crucial for ancestral activity, the HSS motif does not affect other enzymatic properties like structural stability or chemical activity as the promiscuous side activities are present in *Dq1*HSS (motif present) as well as in *la*HSS wild type and mutant proteins (motif absent and present). Promiscuous functions can serve a starting point of evolution (Aharoni et al., 2005; DePristo, 2007). In case of DHS and its duplicates, loss of ancestral function might be an important prerequisite for acquiring or optimizing a new function *in vivo*.

Summarizing, the motif might be indicative for the loss of the DHS activity but it not sufficient to predict the new *in vivo* functions of the gene copy, exemplified by the HSS from *D. quinquefolius* individual 2, that lacks an HSS motif and shows a reduced HSS activity, but still PAs are produced in this individual.

3.3 | Conclusions

HSS catalyzes the first step in PA biosynthesis and has been recruited for this new function after independent duplications of a *dhs* gene in many PA-producing families of the angiosperms. Although putative *hss* gene sequences have been identified that share a common ancestry and that also show high sequence identity in eight morning glory species, PAs have only been found in two species. Thus, to our current knowledge, while a functional HSS is quintessential for PA biosynthesis, the occurrence of an *hss*-like gene does not predict the presence of PAs in such species. This might be attributable to the evolutionary complexity in the recruitment of the duplicated *hss* gene copy into the novel function of PA biosynthesis. The functional relevance of a proposed HSS motif is far from being understood and highlights the mechanistic complexity of protein biochemistry.

4 | METHODS

4.1 | Plant material

All the species used in this study, the source of the seeds, and the analyzed plant parts are summarized in Table S1. The seeds of the plants were germinated on sterile wet filter paper in glass Petri dishes kept in the dark for 2–3 days at room temperature. The seedlings were cultivated in climate chambers (with 16 h light and 8 h dark cycles; temperature 24°C; relative humidity 50%) for a week and then transferred to the green house in Kiel Botanical Gardens (Kiel University). Voucher specimens of *D. quinquefolius* individual 1 and 2, and *J. paniculata* have been deposited in the Herbarium of Kiel University, accession numbers are requested. Samples for PA analyses were taken in the vegetative growth phase. Morphological characters were

used to taxonomically identify the sampled plants, and taxonomic experts confirmed the identifications.

4.2 | Total RNA and genomic DNA isolation

Both, genomic DNA and total RNA, were isolated either from freshly harvested plant tissues or from frozen samples stored at -80°C . Genomic DNA was extracted by using the DNeasy Plant Mini Kit (Qiagen) according to the manufacturer's instructions. Total RNA was isolated by using the RNeasy Plant Mini Kit (Qiagen) or TRIzol reagent (Invitrogen) following the manufacturer's protocols (for further details, see Table S2).

4.3 | cDNA synthesis

One microgram of total RNA was used to synthesize complementary DNA (cDNA) with RevertAid Reverse Transcriptase (ThermoFisher) following the manufacturer's protocol with oligo-dT primer P28 or the oligo-dT primer P39 (Scotto-Lavino et al., 2007a, 2007b) (for further details, see Table S2). Primer sequences are given in Table S3. All oligonucleotides were synthesized at MWG Eurofins Genomics.

4.4 | Amplification of *hss* and *dhs* homologs

Various types of PCR techniques were used to amplify the homologous sequences of *dhs* and *hss* genes in the selected species. The complete amplification strategy is summarized in Table S2. First, we mined online sequence databases for previously published DHS- and HSS-coding sequences of Convolvulaceae. The sequences were aligned by using MAFFT V7.0 software with default values (Kato et al., 2002) installed in the Geneious software package (version 11.0.5, Biomatters). Based on the alignment, conserved regions were used to design the degenerate oligonucleotide primers P1-P4, P16, P27, P29, and P30 (Table S3). These primers were employed to amplify internal fragments of the *dhs* and *hss* homologs from cDNA and/or from genomic DNA. The 5' and 3' regions that flank the internal fragments were amplified by using rapid amplification of cDNA ends (RACE) PCRs (Scotto-Lavino et al., 2007a, 2007b) with cDNA or by applying inverse PCR (Ochman et al., 1988) and FPNI PCR (Wang et al., 2011) techniques with genomic DNA. The resulting PCR products were purified from the PCR mix (NucleoSpin™ Gel and PCR Clean-up, Macherey-Nagel) or extracted after agarose gel electrophoresis (GeneJET™ Gel Extraction Kit, Thermo Scientific) and cloned into the pGEM-T Easy vector (Promega). Resulting constructs were propagated in *Escherichia coli* TOP10 (Thermo Scientific) and sent out for Sanger sequencing (MWG Eurofins Genomics). Assembly of the amplified cDNA sequences and assignment of exonic/intronic regions in genomic sequences were performed with Geneious software packages based on previously characterized sequences of *I. neei* (HSS—HF911505.1; DHS—HF911504.1).

4.5 | Site-directed mutagenesis

The open reading frame of *laHSS*, cloned in an expression vector (Novagen™ pET22a, Millipore Sigma, Billerica, MA, USA, Kaltenecker et al., 2013) with an artificial C-terminal hexahistidine (6xHis) tag extension, was used as template for site-directed mutagenesis guided by (Liu & Naismith, 2008). Primer pairs to introduce the single mutations N266 to H266 (numbering of the amino acids follows Kaltenecker et al., 2013), V277 to I277, and D281 to N281, are given in Table S3. The triple mutant was produced in a two-step process. First, the single mutation N266H was introduced. Second, this plasmid was used as template for PCR with a second primer pair, which introduced the mutations V277I and D281N. PCR amplifications were performed in 25 μl reaction volume with Phusion® High-Fidelity DNA Polymerase (Thermo-Scientific) according to the manufacturer's instructions. Twelve amplification cycles were performed. The PCR products were treated with *DpnI* (Thermo-Scientific) at 37°C for 1 hour, diluted with water (1:10), subsequently propagated in *E. coli* TOP10 (Thermo-Scientific), and sent out for Sanger sequencing (MWG Eurofins Genomics) to identify successful mutants.

4.6 | Gene tree reconstruction

In total, the identified DHS homologs (Table S4) plus DHS encoding sequences from *N. tabacum* (accession number AJ242017) and *S. lycopersicum* L. (syn. *L. esculentum*) (accession number AF296077.1) were analyzed. The latter two sequences were used as outgroup. Furthermore, the DHS encoding sequence from the genome of *C. australis* (accession number RAL37146.1) was included. The open reading frames (ORFs) were aligned by using the MAFFT V7.0 (Kato et al., 2002) algorithm implemented in the Geneious software package (algorithm: G-INS-i; scoring matrix 200PAM/k = 2; gap opening penalty = 1.53; offset value = .123) (Kearse et al., 2012). The resulting multiple sequence alignment was evaluated by using the GUIDANCE2 server (Sela et al., 2015) to remove uncertain alignment positions (below default value of .93). The pairwise identity of nucleotides from the alignment was calculated by means of Geneious (Table 1). A maximum likelihood phylogenetic tree was constructed based on the alignment by using PhyML 3.0 (nucleotide substitution model: GTR + GAMMA; Bootstrapping with 1000 replicates, Guindon et al., 2010) installed in the Geneious software package.

4.7 | Estimation of the amount of pairwise synonymous substitution (Ks)

Codon based alignment based on translated protein sequences using MAFFT V7.0 (Kato et al., 2002) was used to estimate the amount of pairwise synonymous substitution by using the maximum likelihood method implemented in Codeml (Yang, 2007) under the basic model



F3x4 (Goldman & Yang, 1994) by specifying model = 0, NSSites = 0, and runmode = -2.

4.8 | PA extraction from plant tissues

Plant samples were ground to a fine powder by using a laboratory mill (Retsch MM400). 100 μ l heliotrine (1 mg/ml) were added to 100 mg dried plant material as an internal standard. PAs were extracted following Kruse et al. (2017). In short, 2 ml .05 M sulfuric acid was added to 100 mg ground plant material, and the mixture was incubated at room temperature for 2 h to extract PAs. After centrifugation of the solution, the supernatant was treated with zinc to reduce the PA N-oxides to the respective tertiary alkaloids at room temperature for 3 h. The reduced PAs were extracted via Sola CX—mixed mode cation exchanger columns (Thermo-Scientific) following the manufacturer's protocol, except for the replacement of formic acid by .05 M sulfuric acid to ensure maximum compatibility with our sample preparation. PAs were eluted from the columns with 300 μ l methanol including 1% ammonia. To concentrate the PAs in the eluent, the methanol was evaporated under a hood at room temperature, and the dry residue was finally dissolved in 50 μ l methanol for further analysis by GC-MS and GC-FID. The necine bases trachelanthimidine and isoretronecanol in *I. alba* root extracts were identified as trimethylsilyl derivatives using MSTFA as derivatizing reagent according to Hartmann et al. (2005).

4.9 | PA analysis by GC and GC-MS

GC-MS analyses were performed with Thermo TRACE GC ULTRA-DSQ/TRACE GC1310-TSQ Duo equipped with a TraceGOLD™ TG-5MS (30 m \times .25 mm \times .25 μ m; ThermoFisher Scientific, Dreieich, Germany) or TG-1MS capillary columns (30 m \times .25 mm \times .25 μ m; ThermoFisher Scientific, Dreieich, Germany) provided with a 5-M Safeguard guard column. The instrumental specifications were injection volume of 1 μ l and split ratio varying depending on PA concentration of the extracts from splitless (splitless time 1 min) to split 1:10; helium was used as carrier gas with a flow rate of 1 ml min⁻¹ (TRACE GC ULTRA-DSQ) or 1.2 ml min⁻¹ (TRACE GC1310-TSQ); injector and transfer line were set at 280°C and the ion source of the mass spectrometer was operated at 280°C and 70 eV for ionization. The temperature program used was initial 3 min at 100°C, then increasing by 6°C min⁻¹ to 300°C, followed by 10 min at 300°C. The data processing was performed by using Xcalibur™ software (Thermo-Scientific). The internal standard (heliotrine) and PAs were identified via comparison with in-house and literature reference data of mass spectra (El-Shazly & Wink, 2014; Jenett-Siems et al., 2005, 1998; Johnson, 2014, and retention indices). The linear retention indices were calculated with a reference set of co-injected hydrocarbons (Sigma-Aldrich). For quantification of PAs in *D. quinquefolius* individuals, GC-FID analyses with TRACE GC1310 equipped with a TG-1MS capillary column (30 m \times .25 mm \times .25 μ m; ThermoFisher Scientific, Dreieich,

Germany) were performed. The GC conditions applied were identical as described for GC-MS. PAs were quantified via their FID signal relating to heliotrine as internal standard. The 50 μ g heliotrine were added per 100 mg grinded plant powder. The PA amount was calculated as heliotrine equivalents (μ g) per 1 g dry weight of plant material.

4.10 | Heterologous expression, purification and activity assays of HSS encoding cDNAs from *D. quinquefolius* and *C. umbellata*

The complete ORFs of the HSS encoding cDNAs from *D. quinquefolius* individual 1 and 2, and *C. umbellata*, were cloned into the expression vector pET22b (Novagen), expressed in *E. coli* BL21(DE3) and purified according to Ober and Hartmann (Ober & Hartmann, 1999a). HSS from *I. alba* has already been cloned previously (Kaltenegger et al., 2013). Expression constructs were sequenced to ensure correct insertion of the insert. Protein purification was monitored via SDS-PAGE analysis and protein quantities were estimated based on UV absorption at 280 nm and the specific extinction of the respective protein, calculated with the PROTPARAM web tool on EXPASY (Gasteiger et al., 2005). The oligomerization state was analyzed by SEC-MALS-UV. For biochemical characterization, the purified proteins were concentrated and rebuffed to glycine-based (50 mM glycine-NaOH buffer, pH 9) and borate-based (50 mM borate-NaOH buffer, pH 9) assay buffers. Both assay buffers included the additives 1 mM DTT and .1 mM EDTA. The in vitro assay were performed with a newly developed, non-radioactive assay according to Kaltenegger et al. (2021).

In short, 5 to 80 μ g purified recombinant protein were incubated with the acceptor polyamines putrescine, cadaverine, or *N*-methylputrescine together with the donor polyamines spermine or spermidine (400 μ M each), in the presence of NAD (2 mM). Product formation was quantified via derivatizing of the reaction mixture with 9-fluorenylmethyl chloroformate (FMOC, Sigma) and subsequent analyses by HPLC coupled with UV detection. To test DHS activity, enzymes were incubated with the eIF5A precursor protein from *Senecio vernalis*. To detect deoxyhypusine in the in vitro assay with eIF5A precursor protein, the assays were hydrolyzed as described in (Kaltenegger et al., 2021). LC-MS analyses were performed as described in Kaltenegger et al. (2021) and used to confirm the identity of deoxyhypusine and (4-aminobutyl)(5-aminopentyl)amine by their [M + H]⁺ and [M + NH₄]⁺ ions of: 884 and 901; 840 and 857, respectively.

4.11 | Size-exclusion chromatography coupled to multi-angle light scattering (SEC-MALS)

The 20 μ l affinity-purified DHS and HSS samples in glycine or borate buffer with concentrations ranging from 3–7 g·L⁻¹ were separated on an analytical size-exclusion chromatography (SEC)

column (WTC-015N5, equipped with guard column WTC-015N5G; Wyatt Technology) equilibrated with PBS (10 mM Na₂HPO₄, 1.8 mM KH₂PO₄, 137 mM NaCl, 2.7 mM KCl, pH 7.4) and connected to an Agilent Technologies 1100 Series HPLC system (DAD G1315B, RID G1362A) and a miniDAWN TREOS multi-angle light scattering detector (laser beam: 658.9 nm, detectors: 43.6°, 90°, 136.4°; Wyatt Technology). All analyses were run at .4 ml min⁻¹ at room temperature (22°C) for 20 min. Data collection and SEC-MALS analysis was performed with ASTRA V 5.3.4.10 software (Wyatt Technology).

4.12 | Homology modeling of plant DHS and HSS

Homology models of *Distimake quinquefolius* 1 & 2, *I. alba*, *Ipomoea neei* and *Camonea umbellata* DHS and HSS were predicted with the SWISS-MODEL webserver (Waterhouse et al., 2018) based on the structure of human DHS (Tanaka et al., 2020) with bound inhibitor GC7 and NAD ligands (PDB: 6P4V) and analyzed and colored with tools from the UCSF Chimera suite (v.1.15) (Pettersen et al., 2004).

ACKNOWLEDGMENTS

We thank Prof. Tatyana Livshultz for discussions, and we thank Prof. Kirsten Krause for DHS homology analyses of the *Cuscuta campestris* and *C. australis* genome. We thank Prof. Eckart Eich for providing seeds of various species of Convolvulaceae. We also thank Prof. Eckart Eich and Prof. George Staples for additional support with taxonomy. We thank Zhangjun Fei for sharing the information of the location of *dhs* and *hss* gene in synthetic blocks of *I. trifida* and *I. triloba*. We are also grateful to the staff of the Botanical Garden Kiel for their help with the cultivation of plants used in this study. Open Access funding enabled and organized by Projekt DEAL.

CONFLICT OF INTEREST

The authors declare that they have no competing interests.

AUTHOR CONTRIBUTIONS

EK devised the study. EK and A-SP prepared the plant materials for GC-MS analyses. EK and A-SP identified and analyzed the gene sequences. A-RGS authenticated the samples' identification and offered taxonomic support to the study in general. TB, EK, and TS analyzed and interpreted the GC-MS data. SSC analyzed and interpreted LC-MS data. CH performed and interpreted SEC-MALS analyses and homology modeling. EK, A-SP, A-RGS, and DO prepared the figures and wrote, discussed, and edited the manuscript. All authors read and approved the final version. The authors also acknowledge the help of a professional editing service.

DATA AVAILABILITY STATEMENT

The DNA sequences obtained in the current study were submitted to GenBank and are available at NCBI (Table S4). The data sets supporting the conclusions of this article are included within the article (and its supporting information).

ORCID

Ana Rita G. Simões  <https://orcid.org/0000-0001-7267-8353>
 Christina Hopf  <https://orcid.org/0000-0002-6709-6081>
 Serhat Sezai Çiçek  <https://orcid.org/0000-0002-3038-8523>
 Thomas Stegemann  <https://orcid.org/0000-0002-0391-3337>
 Elisabeth Kaltenegger  <https://orcid.org/0000-0001-6542-1509>

REFERENCES

- Afanador, G. A., Tomchick, D. R., & Phillips, M. A. (2018). Trypanosomatid Deoxyhypusine synthase activity is dependent on shared active-site complementation between Pseudoenzyme paralogs. *Structure*, 26(11), 1499, e5–1512. <https://doi.org/10.1016/j.str.2018.07.012>
- Aharoni, A., Gaidukov, L., Khersonsky, O., Gould, S. M., Roodveldt, C., & Tawfik, D. S. (2005). The “evolability” of promiscuous protein functions. *Nature Genetics*, 37(1), 73–76. <https://doi.org/10.1038/ng1482>
- Austin, D. F. (1979). An infrageneric classification for *Ipomoea* (Convolvulaceae). *Taxon*, 28(4), 359–361.
- Beaulieu, W. T., Panaccione, D. G., Quach, Q. N., Smooth, K. L., & Clay, K. (2021). Diversification of ergot alkaloids and heritable fungal symbionts in morning glories. *Communications Biology*, 4(1), 667–678. <https://doi.org/10.1038/s42003-021-02870-z>
- Bershtein, S., Kleiner, D., & Mishmar, D. (2021). Predicting 3D protein structures in light of evolution. *Nature Ecology & Evolution*, 5(9), 1–4. <https://doi.org/10.1038/s41559-021-01519-8>
- Böttcher, F., Ober, D., & Hartmann, T. (1994). Biosynthesis of pyrrolizidine alkaloids: Putrescine and spermidine are essential substrates of enzymatic homospermidine formation. *Canadian Journal of Chemistry*, 72, 80–85. <https://doi.org/10.1139/v94-013>
- Chattopadhyay, M. K., Park, M. H., & Tabor, H. (2008). Hypusine modification for growth is the major function of spermidine in *Saccharomyces cerevisiae* polyamine auxotrophs grown in limiting spermidine. *Proceedings of the National Academy of Sciences of the United States of America*, 105(18), 6554–6559. <https://doi.org/10.1073/pnas.0710970105>
- Chen, G.-T., Lu, Y., Yang, M., Li, J.-L., & Fan, B.-Y. (2018). Medicinal uses, pharmacology, and phytochemistry of Convolvulaceae plants with central nervous system efficacies: A systematic review. *Phytotherapy Research*, 32(5), 823–864. <https://doi.org/10.1002/ptr.6031>
- DePristo, M. A. (2007). The subtle benefits of being promiscuous: Adaptive evolution potentiated by enzyme promiscuity. *Human Frontier Science Program*, 1, 94–98. <https://doi.org/10.2976/1.2754665>
- Dreyer, D. L., Jones, K. C., & Molyneux, R. J. (1985). Feeding deterrence of some pyrrolizidine, indolizidine, and quinolizidine alkaloids towards pea aphid (*Acyrtosiphon pisum*) and evidence for phloem transport of indolizidine alkaloid swainsonine. *Journal of Chemical Ecology*, 11(8), 1045–1051. <https://doi.org/10.1007/BF01020674>
- Eich, E. (2008). *Solanaceae and Convolvulaceae: Secondary metabolites*. Springer. <https://doi.org/10.1007/978-3-540-74541-9>
- El-Shazly, A., & Wink, M. (2014). Diversity of pyrrolizidine alkaloids in the Boraginaceae structures, distribution, and biological properties. *Diversity*, 6, 188–282. <https://doi.org/10.3390/d6020188>
- Eserman, L. A., Tiley, G. P., Jarret, R. L., Leebens-Mack, J. H., & Miller, R. E. (2014). Phylogenetics and diversification of morning glories (tribe Ipomoeae, Convolvulaceae) based on whole plastome sequences. *American Journal of Botany*, 101, 92–103. <https://doi.org/10.3732/ajb.1300207>
- Gasteiger, E., Hoogland, C., Gattiker, A., Duvaud, S., Wilkins, M. R., Appel, R. D., & Bairoch, A. (2005). Protein Identification and Analysis Tools on the ExPASy Server. In *The proteomics protocols handbook* (pp. 571–607). Humana Press. Available at: <https://link.springer.com/protocol/10.1385/1-59259-890-0:571>



- Gill, G. P., Bryant, C. J., Fokin, M., Huege, J., Fraser, K., Jones, C., Cao, M., & Faville, M. J. (2018). Low pyrrolizidine alkaloid levels in perennial ryegrass is associated with the absence of a homospermidine synthase gene. *BMC Plant Biology*, 18, 56. <https://doi.org/10.1186/s12870-018-1269-6>
- Goldman, N., & Yang, Z. (1994). A codon-based model of nucleotide substitution for protein-coding DNA sequences. *Molecular Biology and Evolution*, 11, 725–736. <https://doi.org/10.1093/oxfordjournals.molbev.a040153>
- Gourley, J. M., Heacock, R. A., McInnes, A. G., Nikolin, B., & Smith, D. G. (1969). The structure of ipalbine, a new hexahydroindolizine alkaloid, isolated from *Ipomoea alba* L. *Journal of the Chemical Society D*, (13), 709–710. <https://doi.org/10.1039/c29690000709>
- Guindon, S., Dufayard, J.-F., Lefort, V., Anisimova, M., Hordijk, W., & Gascuel, O. (2010). New algorithms and methods to estimate maximum-likelihood phylogenies: Assessing the performance of PhyML 3.0. *Systematic Biology*, 59, 307–321. <https://doi.org/10.1093/sysbio/syq010>
- Hartmann, T. (1999). Chemical ecology of pyrrolizidine alkaloids. *Planta*, 207, 483–495. <https://doi.org/10.1007/s004250050508>
- Hartmann, T., Biller, A., Witte, L., Ernst, L., & Boppré, M. (1990). Transformation of plant pyrrolizidine alkaloids into novel insect alkaloids by Arctiid moths (Lepidoptera). *Biochemical Systematics and Ecology*, 18(7–8), 549–554. [https://doi.org/10.1016/0305-1978\(90\)90127-2](https://doi.org/10.1016/0305-1978(90)90127-2)
- Hartmann, T., & Ober, D. (2008). Defense by Pyrrolizidine Alkaloids: Developed by Plants and Recruited by Insects. In *Induced plant resistance to herbivory* (pp. 213–231). Springer Science + Business Media B.V. https://doi.org/10.1007/978-1-4020-8182-8_10
- Hartmann, T., Theuring, C., Beuerle, T., Bernays, E. A., & Singer, M. S. (2005). Acquisition, transformation and maintenance of plant pyrrolizidine alkaloids by the polyphagous arctiid *Grammia geneura*. *Insect Biochemistry and Molecular Biology*, 35, 1083–1099. <https://doi.org/10.1016/j.ibmb.2005.05.011>
- Hartmann, T., & Witte, L. (1995). Chemistry, Biology and Chemoecology of the Pyrrolizidine Alkaloids. In *Alkaloids: Chemical and biological perspectives* (pp. 155–233). Elsevier. Available at: <https://linkinghub.elsevier.com/retrieve/pii/B9780080420899500115> Accessed January 5, 2021
- Irmer, S., Podzun, N., Langel, D., Heidemann, F., Kaltenecker, E., Schemmerling, B., Geilfus, C.-M., Zöhr, C., & Ober, D. (2015). New aspect of plant-rhizobia interaction: Alkaloid biosynthesis in *Crotalaria* depends on nodulation. *Proceedings. National Academy of Sciences. United States of America*, 112, 4164–4169. <https://doi.org/10.1073/pnas.1423457112>
- Jenett-Siems, K., Kaloga, M., & Eich, E. (1993). Ipangulines, the first pyrrolizidine alkaloids from the Convolvulaceae. *Phytochemistry*, 34(2), 437–440. [https://doi.org/10.1016/0031-9422\(93\)80025-N](https://doi.org/10.1016/0031-9422(93)80025-N)
- Jenett-Siems, K., Ott, S. C., Schimming, T., Siems, K., Müller, F., Hilker, M., Witte, L., Hartmann, T., Austin, D. F., & Eich, E. (2005). Ipangulines and minalobines, chemotaxonomic markers of the infrageneric *Ipomoea* taxon subgenus Quamoclit, section Mina. *Phytochemistry*, 66, 223–231. <https://doi.org/10.1016/j.phytochem.2004.11.019>
- Jenett-Siems, K., Schimming, T., Kaloga, M., Eich, E., Siems, K., Gupta, M. P., Witte, L., & Hartmann, T. (1998). Pyrrolizidine alkaloids of *Ipomoea hederifolia* and related species. *Phytochemistry*, 47(8), 1551–1560. [https://doi.org/10.1016/S0031-9422\(97\)01082-0](https://doi.org/10.1016/S0031-9422(97)01082-0)
- Jiao, Y., Li, J., Tang, H., & Paterson, A. H. (2014). Integrated Syntenic and Phylogenomic analyses reveal an ancient genome duplication in monocots. *Plant Cell*, 26(7), 2792–2802. <https://doi.org/10.1105/tpc.114.127597>
- Joe, Y. A., Wolff, E. C., Lee, Y. B., & Park, M. H. (1997). Enzyme-substrate intermediate at a specific lysine residue is required for Deoxyhypusine synthesis. *The Journal of Biological Chemistry*, 272, 32679–32685. <https://doi.org/10.1074/jbc.272.51.32679>
- Johnson, S.G. (2014) NIST Standard Reference Database 1A v17. NIST. Available at: <https://www.nist.gov/srd/nist-standard-reference-database-1a-v17>
- Kaltenecker, E., Eich, E., & Ober, D. (2013). Evolution of Homospermidine synthase in the Convolvulaceae: A story of gene duplication, gene loss, and periods of various selection pressures. *Plant Cell*, 25(4), 1213–1227. <https://doi.org/10.1105/tpc.113.109744>
- Kaltenecker, E., & Ober, D. (2015). Paralogous interference affects the dynamics after gene duplication. *Trends in Plant Science*, 20, 814–821. <https://doi.org/10.1016/j.tplants.2015.10.003>
- Kaltenecker, E., Prakashrao, A. S., Çiçek, S. S., & Ober, D. (2021). Development of an activity assay for characterizing deoxyhypusine synthase and its diverse reaction products. *FEBS Open Bio*, 11, 10–25. <https://doi.org/10.1002/2211-5463.13046>
- Kaltner, F., Rychlik, M., Gareis, M., & Gottschalk, C. (2018). Influence of storage on the stability of toxic pyrrolizidine alkaloids and their N-oxides in peppermint tea, Hay, and honey. *Journal of Agricultural and Food Chemistry*, 66, 5221–5228. <https://doi.org/10.1021/acs.jafc.7b06036>
- Katoh, K., Misawa, K., Kuma, K., & Miyata, T. (2002). MAFFT: A novel method for rapid multiple sequence alignment based on fast Fourier transform. *Nucleic Acids Research*, 30, 3059–3066. <https://doi.org/10.1093/nar/gkf436>
- Kearse, M., Moir, R., Wilson, A., Stones-Havas, S., Cheung, M., Sturrock, S., Buxton, S., Cooper, A., Markowitz, S., Duran, C., Thierer, T., Ashton, B., Meintjes, P., & Drummond, A. (2012). Geneious basic: An integrated and extendable desktop software platform for the organization and analysis of sequence data. *Bioinformatics*, 28(12), 1647–1649. <https://doi.org/10.1093/bioinformatics/bts199>
- Koonin, E. V. (2016). Splendor and misery of adaptation, or the importance of neutral null for understanding evolution. *BMC Biology*, 14, 114. Available at: <http://www.ncbi.nlm.nih.gov/pmc/articles/PMC5180405/>; <https://doi.org/10.1186/s12915-016-0338-2>
- Kruse, L. H., Stegemann, T., Sievert, C., & Ober, D. (2017). Identification of a second site of pyrrolizidine alkaloid biosynthesis in comfrey to boost plant defense in floral stage. *Plant Physiology*, 174, 47–55. <https://doi.org/10.1104/pp.17.00265>
- Langel, D., Ober, D., & Pelsler, P. B. (2011). The evolution of pyrrolizidine alkaloid biosynthesis and diversity in the Senecioneae. *Phytochemistry Reviews*, 10, 3–74. <https://doi.org/10.1007/s11101-010-9184-y>
- Leistner, E., & Steiner, U. (2018). The Genus *Periglandula* and Its Symbiont with Morning Glory Plants (Convolvulaceae). In T. Anke & A. Schüffler (Eds.), *Physiology and genetics: Selected basic and applied aspects* (pp. 131–147). Available at: Springer International Publishing. https://doi.org/10.1007/978-3-319-71740-1_5
- Liu, H., & Naismith, J. H. (2008). An efficient one-step site-directed deletion, insertion, single and multiple-site plasmid mutagenesis protocol. *BMC Biotechnology*, 8(1), 91. <https://doi.org/10.1186/1472-6750-8-91>
- Livshultz, T., Kaltenecker, E., Straub, S. C. K., Weitemier, K., Hirsch, E., Khrystyna, K., Lumi, M., & Aaron, L. (2018). Evolution of pyrrolizidine alkaloid biosynthesis in Apocynaceae: Revisiting the defence de-escalation hypothesis. *New Phytologist*, 218, 762–773. <https://doi.org/10.1111/nph.15061>
- Lynch, M., & Conery, J. S. (2000). The evolutionary fate and consequences of duplicate genes. *Science*, 290(5494), 1151–1155. <https://doi.org/10.1126/science.290.5494.1151>
- Macel, M., Vrieling, K., & Klinkhamer, P. G. L. (2004). Variation in pyrrolizidine alkaloid patterns of *Senecio jacobaea*. *Phytochemistry*, 65(7), 865–873. <https://doi.org/10.1016/j.phytochem.2004.02.009>
- Mann, P. (1997). *Zur Phytochemie und Chemotaxonomie tropischer und mediterranean Convolvulaceen unter besonderer Berücksichtigung des Alkaloid-Vorkommens*. Freie Universität Berlin.
- Muñoz-Rodríguez, P., Carruthers, T., Wood, J. R. I., Williams, B. R. M., Weitemier, K., Kronmiller, B., Goodwin, Z., Sumadijaya, A.,

- Anglin, N. L., Filer, D., Harris, D., Rausher, M. D., Kelly, S., Liston, A., & Scotland, R. W. (2019). A taxonomic monograph of *Ipomoea* integrated across phylogenetic scales. *Nature Plants*, 5, 1136–1144. <https://doi.org/10.1038/s41477-019-0535-4>
- Ober, D., & Hartmann, T. (1999a). Deoxyhypusine synthase from tobacco cDNA isolation, characterization, and bacterial expression of an enzyme with extended substrate specificity. *The Journal of Biological Chemistry*, 274, 32040–32047. <https://doi.org/10.1074/jbc.274.45.32040>
- Ober, D., & Hartmann, T. (1999b). Homospermidine synthase, the first pathway-specific enzyme of pyrrolizidine alkaloid biosynthesis, evolved from deoxyhypusine synthase. *Proceedings. National Academy of Sciences. United States of America*, 96, 14777–14782. <https://doi.org/10.1073/pnas.96.26.14777>
- Ober, D., Gibas, L., Witte, L., & Hartmann, T. (2003). Evidence for general occurrence of homospermidine in plants and its supposed origin as by-product of deoxyhypusine synthase. *Phytochemistry*, 62, 339–344. [https://doi.org/10.1016/S0031-9422\(02\)00553-8](https://doi.org/10.1016/S0031-9422(02)00553-8)
- Ober, D., Harms, R., Witte, L., & Hartmann, T. (2003). Molecular evolution by change of function. *The Journal of Biological Chemistry*, 278, 12805–12812. <https://doi.org/10.1074/jbc.M207112200>
- Ochman, H., Gerber, A. S., & Hartl, D. L. (1988). Genetic applications of an inverse polymerase chain reaction. *Genetics*, 120(3), 621–623. <https://doi.org/10.1093/genetics/120.3.621>
- OMaille, P. E., Malone, A., Dellas, N., O'Maille, P. E., Andes Hess, B. Jr., Smentek, L., Sheehan, I., Greenhagen, B. T., Chappell, J., Manning, G., & Noel, J. P. (2008). Quantitative exploration of the catalytic landscape separating divergent plant sesquiterpene synthases. *Nature Chemical Biology*, 4(10), 617–623. <https://doi.org/10.1038/nchembio.113>
- Panaccione, D. G., Beaulieu, W. T., & Cook, D. (2014). Bioactive alkaloids in vertically transmitted fungal endophytes. *Functional Ecology*, 28, 299–314. <https://doi.org/10.1111/1365-2435.12076>
- Panchy, N., Lehti-Shiu, M., & Shiu, S.-H. (2016). Evolution of gene duplication in plants. *Plant Physiology*, 171, 2294–2316. <https://doi.org/10.1104/pp.16.00523>
- Park, J.-H., Wolff, E. C., Folk, J. E., & Park, M. H. (2003). Reversal of the Deoxyhypusine synthesis reaction. *The Journal of Biological Chemistry*, 278, 32683–32691. <https://doi.org/10.1074/jbc.M304247200>
- Paulke, A., Kremer, C., Wunder, C., Achenbach, J., Djahanschiri, B., Elias, A., Stefan Schwed, J., Hübner, H., Gmeiner, P., Proschak, E., Toennes, S. W., & Stark, H. (2013). *Argyria nervosa* (Burm. F.): Receptor profiling of lysergic acid amide and other potential psychedelic LSD-like compounds by computational and binding assay approaches. *Journal of Ethnopharmacology*, 148, 492–497. <https://doi.org/10.1016/j.jep.2013.04.044>
- Petterson, E. F., Goddard, T. D., Huang, C. C., Couch, G. S., Greenblatt, D. M., Meng, E. C., & Ferrin, T. E. (2004). UCSF chimera—A visualization system for exploratory research and analysis. *Journal of Computational Chemistry*, 25(13), 1605–1612. <https://doi.org/10.1002/jcc.20084>
- Qiao, X., Li, Q., Yin, H., Qi, K., Li, L., Wang, R., Zhang, S., & Paterson, A. H. (2019). Gene duplication and evolution in recurring polyploidization–diploidization cycles in plants. *Genome Biology*, 20(1), 38. <https://doi.org/10.1186/s13059-019-1650-2>
- Rausher, M. D., Miller, R. E., & Tiffin, P. (1999). Patterns of evolutionary rate variation among genes of the anthocyanin biosynthetic pathway. *Molecular Biology and Evolution*, 16, 266–274. <https://doi.org/10.1093/oxfordjournals.molbev.a026108>
- Reimann, A., Nurhayati, N., Backenköhler, A., & Ober, D. (2004). Repeated evolution of the pyrrolizidine alkaloid–mediated defense system in separate angiosperm lineages. *Plant Cell*, 16(10), 2772–2784. <https://doi.org/10.1105/tpc.104.023176>
- Reinhard, A., Janke, M., von der Ohe, W., Kempf, M., Theuring, C., Hartmann, T., Schreier, P., & Beuerle, T. (2009). Feeding deterrence and detrimental effects of pyrrolizidine alkaloids fed to honey bees (*Apis mellifera*). *Journal of Chemical Ecology*, 35(9), 1086–1095. <https://doi.org/10.1007/s10886-009-9690-9>
- Schardl, C. L., Grossman, R. B., Nagabhyyu, P., Faulkner, J. R., & Mallik, U. P. (2007). Loline alkaloids: Currencies of mutualism. *Phytochemistry*, 68(7), 980–996. <https://doi.org/10.1016/j.phytochem.2007.01.010>
- Scotto-Lavino, E., Du, G., & Frohman, M. A. (2007a). 3' end cDNA amplification using classic RACE. *Nature Protocols*, 1(6), 2742–2745. <https://doi.org/10.1038/nprot.2006.481>
- Scotto-Lavino, E., Du, G., & Frohman, M. A. (2007b). 5' end cDNA amplification using classic RACE. *Nature Protocols*, 1(6), 2555–2562. <https://doi.org/10.1038/nprot.2006.480>
- Sela, I., Ashkenazy, H., Katoh, K., & Pupko, T. (2015). GUIDANCE2: Accurate detection of unreliable alignment regions accounting for the uncertainty of multiple parameters. *Nucleic Acids Research*, 43, W7–W14. <https://doi.org/10.1093/nar/gkv318>
- Simões, A. R., Culham, A., & Carine, M. (2015). Resolving the unresolved tribe: A molecular phylogenetic framework for the Merremieae (Convolvulaceae). *Botanical Journal of the Linnean Society*, 179, 374–387. <https://doi.org/10.1111/boj.12339>
- Simões, A. R., & Staples, G. (2017). Dissolution of Convolvulaceae tribe Merremieae and a new classification of the constituent genera. *Botanical Journal of the Linnean Society*, 183(4), 561–586. <https://doi.org/10.1093/botlinnean/box007>
- Stefanović, S., Austin, D. F., & Olmstead, R. G. (2003). Classification of Convolvulaceae: A phylogenetic approach. *Systematic Botany*, 28, 791–806.
- Stefanovic, S., Krueger, L., & Olmstead, R. G. (2002). Monophyly of the Convolvulaceae and circumscription of their major lineages based on DNA sequences of multiple chloroplast loci. *American Journal of Botany*, 89(9), 1510–1522. <https://doi.org/10.3732/ajb.89.9.1510>
- Sun, G., Xu, Y., Liu, H., Sun, T., Zhang, J., Hettenhausen, C., Shen, G., Qi, J., Qin, Y., Li, J., Wang, L., Chang, W., Guo, Z., Baldwin, I. T., & Wu, J. (2018). Large-scale gene losses underlie the genome evolution of parasitic plant *Cuscuta australis*. *Nature Communications*, 9(1), 2683. <https://doi.org/10.1038/s41467-018-04721-8>
- Tanaka, Y., Kurasawa, O., Yokota, A., Klein, M. G., Ono, K., Saito, B., Matsumoto, S., Okaniwa, M., Ambrus-Aikelin, G., Morishita, D., Kitazawa, S., Uchiyama, N., Ogawa, K., Kimura, H., & Imamura, S. (2020). Discovery of novel allosteric inhibitors of Deoxyhypusine synthase. *Journal of Medicinal Chemistry* Available at, 63, 3215–3226. <https://doi.org/10.1021/acs.jmedchem.9b01979>
- Tofern, B. (1999). *Neue und seltene Sekundärstoffe des Phenylpropan-, Terpen- und Alkaloid-Stoffwechsels aus tropischen Convolvulaceae*. Freie Universität Berlin.
- Tofern, B., Kaloga, M., Witte, L., Hartmann, T., & Eich, E. (1999). Occurrence of loline alkaloids in *Argyria mollis* (Convolvulaceae). *Phytochemistry*, 51(8), 1177–1180. [https://doi.org/10.1016/S0031-9422\(99\)00121-1](https://doi.org/10.1016/S0031-9422(99)00121-1)
- Umland, T. C., Wolff, E. C., Park, M. H., & Davies, D. R. (2004). A new crystal structure of Deoxyhypusine synthase reveals the configuration of the active enzyme and of an enzyme-NAD-inhibitor ternary complex. *The Journal of Biological Chemistry*, 279, 28697–28705. <https://doi.org/10.1074/jbc.M404095200>
- van Dam, N. M., van der Meijden, E., & Verpoorte, R. (1993). Induced responses in three alkaloid-containing plant species. *Oecologia*, 95(3), 425–430. <https://doi.org/10.1007/BF00320998>
- Vanneste, K., Baele, G., Maere, S., & Peer, Y. V. d. (2014). Analysis of 41 plant genomes supports a wave of successful genome duplications in association with the cretaceous–Paleogene boundary. *Genome Research*, 24(8), 1334–1347. <https://doi.org/10.1101/gr.168997.113>
- Wang, X., Wang, J., Jin, D., Guo, H., Lee, T.-H., Liu, T., & Paterson, A. H. (2015). Genome alignment spanning major Poaceae lineages reveals



- heterogeneous evolutionary rates and alters inferred dates for key evolutionary events. *Molecular Plant*, 8(6), 885–898. <https://doi.org/10.1016/j.molp.2015.04.004>
- Wang, Z., Ye, S., Li, J., Zheng, B., Bao, M., & Ning, G. (2011). Fusion primer and nested integrated PCR (FPNI-PCR): A new high-efficiency strategy for rapid chromosome walking or flanking sequence cloning. *BMC Biotechnology*, 11, 109. <https://doi.org/10.1186/1472-6750-11-109>
- Waterhouse, A., Bertoni, M., Bienert, S., Studer, G., Tauriello, G., Gumienny, R., Heer, F. T., de Beer, T. A. P., Rempfer, C., Bordoli, L., Lepore, R., & Schwede, T. (2018). SWISS-MODEL: Homology modelling of protein structures and complexes. *Nucleic Acids Research*, 46(W1), W296–W303. <https://doi.org/10.1093/nar/gky427>
- Wątor, E., Wilk, P., & Grudnik, P. (2020). Half way to Hypusine—Structural basis for substrate recognition by human Deoxyhypusine synthase. *Biomolecules*, 10(4), 522. <https://doi.org/10.3390/biom10040522>
- WCVP. (2021) World Checklist of Vascular Plants, version 2.0. *Facilitated by the Royal Botanic Gardens, Kew*. Available at: <http://wcvp.science.kew.org/>
- Wesseling, A.-M., Demetrowitsch, T. J., Schwarz, K., & Ober, D. (2017). Variability of pyrrolizidine alkaloid occurrence in species of the grass subfamily Pooideae (Poaceae). *Frontiers in Plant Science*, 8, 2046. <https://doi.org/10.3389/fpls.2017.02046>
- Wiedenfeld, H., & Edgar, J. (2011). Toxicity of pyrrolizidine alkaloids to humans and ruminants. *Phytochemistry Reviews*, 10, 137–151. <https://doi.org/10.1007/s11101-010-9174-0>
- Wolff, E. C., Folk, J. E., & Park, M. H. (1997). Enzyme-substrate intermediate formation at lysine 329 of human Deoxyhypusine synthase. *The Journal of Biological Chemistry*, 272, 15865–15871. <https://doi.org/10.1074/jbc.272.25.15865>
- Wolff, E. C., Park, M. H., & Folk, J. E. (1990). Cleavage of spermidine as the first step in deoxyhypusine synthesis. The Role of NAD. *Journal of Biological Chemistry*, 265, 4793–4799. [https://doi.org/10.1016/S0021-9258\(19\)34042-6](https://doi.org/10.1016/S0021-9258(19)34042-6)
- Yang, X., Gao, S., Guo, L., Wang, B., Jia, Y., Zhou, J., Che, Y., Jia, P., Lin, J., Xu, T., Sun, J., & Ye, K. (2021). Three chromosome-scale *Papaver* genomes reveal punctuated patchwork evolution of the morphinan and noscapine biosynthesis pathway. *Nature Communications*, 12, 6030. <https://doi.org/10.1038/s41467-021-26330-8>
- Yang, Z. (2007). PAML 4: Phylogenetic analysis by maximum likelihood. *Molecular Biology and Evolution*, 24(8), 1586–1591. <https://doi.org/10.1093/molbev/msm088>
- Zakaria, M. M., Schemmerling, B., & Ober, D. (2021). CRISPR/Cas9-mediated genome editing in comfrey (*Symphytum officinale*) hairy roots results in the complete eradication of pyrrolizidine alkaloids. *Molecules*, 26(6), 1498. <https://doi.org/10.3390/molecules26061498>
- Zakaria, M. M., Stegemann, T., Sievert, C., Kruse, L. H., Kaltenecker, E., Girreiser, U., Çiçek, S. S., Nimtz, M., & Ober, D. (2022). Insights into polyamine metabolism: Homospermidine is double-oxidized in two discrete steps by a single copper-containing amine oxidase in pyrrolizidine alkaloid biosynthesis. *The Plant Cell*, 34(6), 2364–2382. <https://doi.org/10.1093/plcell/koac068>

SUPPORTING INFORMATION

Additional supporting information can be found online in the Supporting Information section at the end of this article.

How to cite this article: Prakashrao, A. S., Beuerle, T., Simões, A. R. G., Hopf, C., Çiçek, S. S., Stegemann, T., Ober, D., & Kaltenecker, E. (2022). The long road of functional recruitment—The evolution of a gene duplicate to pyrrolizidine alkaloid biosynthesis in the morning glories (Convolvulaceae). *Plant Direct*, 6(7), e420. <https://doi.org/10.1002/pld3.420>